Gravitational Lorentz Violations in 5D Black Hole Background: A Numerical Investigation

Luis Valcárcel
Centre for High Energy Physics
Department of Physics
McGill University
Montréal, Québec
Canada

August, 2003

A Thesis submitted to
McGill University
in partial fulfillment of the requirements for the degree of
Master of Science

Your file Votre référence
ISBN: 0-612-98756-6
Our file Notre référence
ISBN: 0-612-98756-6

CONTENTS

List of Figures

Abstract

The warped braneworld picture introduced by Randall and Sundrum provides new ways of solving long-standing problems in physics, like the gauge hierarchy problem. If the warp factor is different for the time and space components of the metric, new effects may arise. We concentrate on this possibility and show that the speed of gravity may differ from that of electromagnetism, while Lorentz invariance is preserved for the standard model fields. A charged black hole in a 5 dimensional bulk provides the necessary background. Its properties are studied in detail to ensure correct embedding of the brane. Computation of the speed of gravity in this setup is done both perturbatively and numerically. The results are compared with experimental bounds to constrain the parameters of our scenario.

Résumé

Le scénario de monde branaire introduit par Randall et Sundrum procure de nouvelles voies pour résoudre certains problèmes difficiles en physique, comme celui de la hiérarchie de jauge. Si les facteurs multipliant les parties temporelle et spatiale de la métrique diffèrent, de nouveaux effets apparaissent. On démontre que la vitesse de propagation de la gravité peut être différente de celle de l'électromagnétisme, tout en préservant l'invariance de Lorentz pour les champs du modèle standard. Un trou noir chargé, dans un espace à 5 dimensions, est à la base de notre modèle. Ses propriétés sont étudiées dans le détail pour assurer l'insertion correcte de notre brane. La vitesse de la gravité est calculée de manière perturbative, puis numérique. Les résultats sont confrontés aux limites expérimentales pour contraindre les paramètres de notre scénario.

Acknowledgments

The writing of this thesis is the result of two years of continual efforts. The road has been long and tortuous and I wish to express my gratitude to all of those who provided support along the way.

First, I would like to thank my supervisor Professor J. M. Cline for introducing me to the field of research of phenomenological cosmology. He helped me make my first steps at the graduate studies level and is therefore directly responsible for me attaining my goal. He provided numerous answers to my questions and made several helpful suggestions and comments.

Next, I would like to thank the members of our group. Dr. Hassan Firouzjahi helped me understand the jump conditions of the metric, he also provided help for the understanding of the Randall-Sundrum scenario and he made several suggestions at times when I had troubles with a difficult equation. Julie Descheneau has been a great colleague. We learned the basics of braneworlds together and I am grateful to her for numerous conversations. Her curiosity and vivacity really motivated me to learn more, either not to feel too far behind her or to answer a question she might have had. Joel Trudeau provided help at an early stage with the numerical computation. He got me on the right track from the start. Aaron Berndsen provided the template for the formatting of this thesis. I'm thankful to the rest of the group for their listening and questions during the group meetings. Thanks also go to Professor G. D. Moore for an insightful explanation about the gravi-Čerenkov radiation effect and for many useful comments about other experimental bounds on the speed of gravity.

Last but not least, I would like to thank my friends and family for their continuous moral support. Their presence alleviates the weight of my studies. Special thanks to my brother Carlos Valcárcel for letting me perform long calculations on his computer and to my girlfriend Josianne Lefebvre who encouraged me endlessly during the process and helped me review the final version of this work.

Statement of Original Contributions

The material presented in chapters 2 and 3 is mostly based on the study of [5] and contains some elements that review the works of [3, 4, 17, 37]. However, the study for the parameter space of the regulator brane, presented in section 2.5 and complemented in appendix A is the author's own work. Equally is the extension of the perturbation method to the excited states in section 3.2.2. The numerical calculations presented in chapter 4 were all performed by the author. Chapter 5 discusses various experimental bounds obtained from other works which are cited in this section. The application of these bounds to our case is also an original contribution, but the discussion in that section was alimented by the comments of G. D. Moore. All of the novelties presented in this thesis have benefited from suggestions made by J. M. Cline.

Gravitational Lorentz Violations in 5D Black Hole Background:
A Numerical Investigation

1

Introduction

Attempts at unifying the fundamental forces of nature led physicists to try to formulate what is known as M-theory, which is a theory that postulates that we live in a world of higher dimensions than the usual four we know. This intriguing possibility motivated numerous investigations on how the extra dimensions could have remained hidden from our senses until today. A first idea, known as the Kaluza-Klein (KK) picture, is that they are rolled up in a very tiny space. The effective four-dimensional theory would then be recovered on distances larger than the compactification scale. In this picture, the extra dimensions would need to be so small that it would be impossible to probe them.

Recently, however, a new idea for hiding the extra dimensions, the braneworld picture, provided hope that they would be more accessible to our experiments. Here, the standard model (SM) particles are assumed to be trapped on a (3+1) submanifold of the higher dimensional spacetime, known as a 3-brane. Only gravity, being the fabric of spacetime itself, is not confined to the brane and can therefore probe the extra-dimensions. Since ordinary matter cannot escape into the bulk, it is no longer necessary that the extra-dimensions be microscopic, and it is possible that some effects may become observable. Braneworlds provoked excitement among the community because they offered new possibilities for solving long-standing problems in physics. In such a context, for example, resolutions of the gauge hierarchy problem and of the cosmological constant problem have been attempted.

In the braneworld referred to as ADD [1, 2], the Kaluza-Klein idea is reintroduced by considering compact extra-dimensions. Only this time, since only gravity can feel the extra-dimensions, these need just be smaller than the current distance scale on which gravity has been tested so far. This means that, for the case of two extra-dimensions (the case with one extra-dimension is ruled out in this scenario), their size could be on the submillimetric scale. This picture, although interesting, remains disappointing in the end because it merely recasts the hierarchy problem into another form. Instead of asking why the electroweak scale is so different from the Planck scale, we now ask why is there a hierarchy between the fundamental scale and the compactification scale.

Another braneworld scenario, more interesting than the previous one, is that of Randall and Sundrum (RS) in five dimensions [3, 4]. The key difference is that here it is not assumed that the metric must be factorisable. Instead, a warped metric, of the form

$$ds^2 = a^2(y)\eta_{\mu\nu}dx^\mu dx^\nu + dy^2, \tag{1.1}$$

is used, implying curvature along the extra dimensions. It is the presence of the warp factor $a(y)$ that can provide an exponential hierarchy. What is more, this metric can reproduce 4D gravity with negligible corrections, even if the extra dimension is infinite. Scenarios of this type were studied with much interest with regards to the cosmology and as a potential model to solve the above mentioned problems. From those studies it was realized that there were cases where global Lorentz invariance was violated along the extra dimension [5]-[14]. This manifested itself as different propagation speeds between gravity and electromagnetism, and implied the possibility of seeing what would be interpreted as an acausal signal from the point of view of an observer on the 3-brane. For instance, gravitons emitted from an event would have the possibility to take a shortcut through the bulk and outrun the photon signal stuck on the brane. The gravitational event could be detected before the electromagnetic one. But from the 5D perspective this is no real violation of causality. It is this kind of effect that is the subject of this study.

The present work is heavily inspired by the study of Csáki, Erlich and Grojean, described in [5], where a charged black hole in the bulk is a source of asymmetry in the metric. We wish to confirm their results for the graviton zero mode and extend them to the excited states. Our motivation is that by studying the maximal attainable velocities of the massive states it might be possible to develop a formalism, similar to that of Coleman and Glashow in [15], appropriate to discuss the decays of the particles and to deduce possible signatures for extra-dimensions. Note, however, that the nature of gravitational Lorentz violations is fundamentally different from that of the Lorentz violating effects discussed in [15, 16], it is only the framework for discussing the decays that could present some similarities. We thus follow in the footsteps of Csáki, Erlich and Grojean but we use a numerical approach where they used a perturbation method. This will allow us to verify their model and investigate its limits by studying large perturbations as well. We also want to see if the effect they found could reverse, *i.e.* if the gravitational signal could arrive, at the observer on the 3-brane, later than the light signal. Ultimately, we want to deduce some constraints on the model by applying existing bounds on the effect.

In section 2, we begin by describing what is meant by an asymmetrical spacetime and how this leads to violation of Lorentz invariance. We then specialize the metric to that of a charged black hole in the bulk. The embedding of the brane in the spacetime is discussed and it is shown that a regulator brane is needed to hide the otherwise naked singularity. The properties of the physical brane and of the regulator brane are investigated. In section 3, we review the perturbation method of Csáki, Erlich and Grojean for the zero mode of the graviton. We first solve the unperturbed problem, *i.e.* we find the wave functions of the gravitons in the RS background. Then a small perturbation of the metric functions is introduced and we try to solve for the perturbed wave functions. For the zero mode, the result of [5] is recovered. We extend the method to include the excited states of the graviton. Section 4 discusses the numerical solution of the problem. It is verified that the perturbative approach yields reasonable results for small perturbations. Larger perturbations are examined. The results are put in perspective with experimental bounds in section 5. Our findings are summarized in section 6. Finally, an appendix describes the use of an alternate choice of parameters.

2

The Setup

In this section, we describe the scenario needed to obtain violation of Lorentz invariance. Before describing the spacetime as such, let us explain the phenomenon on general grounds, and the properties that the metric should possess for this to be possible. Then, we will settle on a definite scenario that will be the main subject of this investigation.

2.1 *Modified Dispersion Relation*

Consider the following generic 5D metric for static 3D rotational invariant spacetimes:

$$ds^2 = -n^2(r)dt^2 + a^2(r)d\Sigma_{\tilde{k}}^2 + b^2(r)dr^2, \tag{2.1}$$

where

r	is the extra dimension;
$d\Sigma_{\tilde{k}}^2$	is the spatial 3-section metric, with curvature $\tilde{k} = \pm 1, 0$;
$n(r), a(r), b(r)$	are unspecified metric functions.

Here, and in the remainder of this work, the curvature parameter $\tilde{k}$ is taken to be 0 since we care mostly about a flat space universe (so $d\Sigma_{\tilde{k}}^2 = d\vec{x}^2$). This metric is not only warped (meaning that the coefficients multiplying the 4D section are a function of the extra dimension) like in the RS scenario (see [3] and [4]), it is asymmetrically warped, *i.e.* the warp factors $n(r)$ and $a(r)$ are different. Therefore, the local speed of light $c(r) = \frac{n(r)}{a(r)}$, which we get by setting $ds^2 = 0$ for lightlike particles and $dr^2 = 0$ for particles confined to a 3-brane, is a function of the extra dimension and will vary with position along it. Each 4D section has a different Lorentz symmetry and thus Lorentz invariance is globally broken. Note that we can rescale the t and $\vec{x}$ coordinates so that at r_0, the position of our brane, we have $n(r_0) = a(r_0) = 1$ and the standard model particles restricted there still see the usual Minkowski metric. On the other hand, particles whose wave function has a finite extent in the extra dimension, like the graviton in RSII, get affected by the change in the speed of propagation. Following an example from [17], consider a scalar field Φ which is used to represent the graviton since it has the same equations of motion, see [18]. Its action is

$$S_\Phi = \int dt\, d^3x\, dr \sqrt{|g|} \left[\frac{1}{2} g^{AB} \partial_A \Phi \partial_B \Phi\right]. \tag{2.2}$$

where $g := \det g_{AB} = -n^2(r)a^6(r)b^2(r)$ for the metric in (2.1).

Expanding $S_\Phi := \int d^5x \mathcal{L}(\Phi, \partial_A \Phi)$ in this background, it is easy to see that the Lagrangian density is

$$\mathcal{L} = \frac{n(r)a^3(r)b(r)}{2} \left[\frac{-1}{n^2(r)}(\partial_t\Phi)^2 + \frac{1}{a^2(r)}(\partial_i\Phi)^2 + \frac{1}{b^2(r)}(\partial_r\Phi)^2\right]. \tag{2.3}$$

Applying the Euler-Lagrange procedure to get the equation of motion for this field yields

$$\frac{a^3(r)b(r)}{n(r)}\partial_{tt}\Phi = n(r)a(r)b(r)\partial_{ii}\Phi + \partial_r\left(\frac{n(r)a^3(r)}{b(r)}\partial_r\Phi\right) = 0 \tag{2.4}$$

Now, we assume that this problem can be solved by separation of variables $\Phi(t, \vec{x}, r) = A(t)B(\vec{x})\phi(r)$. Since none of the coefficients has a dependence on t or $\vec{x}$, the differential equations for $A(t)$ and $B(\vec{x})$ are trivial and their solutions can be written as plane waves on the brane; the solution has the form $\Phi(t, \vec{x}, r) = \phi(r)e^{i(\omega t - \vec{q}x)}$, where $\vec{q}$ is the 3-momentum, and ω the energy. With this form, the equation of motion becomes

$$\frac{a^3(r)b(r)}{n(r)}\omega^2\phi(r) = n(r)a(r)b(r)\vec{q}^{\,2}\phi(r) + H^{(0)}(r)\phi(r), \tag{2.5}$$

where

$$H^{(0)}(r) := -\partial_r\left(\frac{n(r)a^3(r)}{b(r)}\partial_r\right) \tag{2.6}$$

is a Hermitian operator. Equation (2.5) is an eigenvalue equation for ω^2. Let us label the eigenfunctions by $\phi_n(r)$. The aim here is to show that solving this equation implies a modification to the usual dispersion relation

$$\omega_n^2 = M_n^2 + \vec{q}^{\,2}, \tag{2.7}$$

where M_n is the mass of the n^{th} excited mode of the particle.

There are two ways to solve this equation approximatively by perturbation techniques. One of them involves perturbing the background metric and will be discussed in detail in section 3 when the explicit form of the metric functions $n(r), a(r)$ and $b(r)$ will be known. For the moment, just to illustrate that the dispersion relation gets modified, let us take the 3-momentum as the perturbation, which we will write as $\lambda n(r)a(r)b(r)\vec{q}^2$ (here λ is used only as a device to keep track of the order of the corrections). We assume that the unperturbed problem

$$H^{(0)}(r)\phi_n^{(0)}(r) = \frac{a^3(r)b(r)}{n(r)}(\omega_n^{(0)})^2\phi_n^{(0)}(r) \tag{2.8}$$

is solved, which means that the eigenfunctions $\phi_n^{(0)}(r)$ and their corresponding eigenvalues $(\omega_n^{(0)})^2$, which we define to be M_n^2, are known. We further assume that the solution to the perturbed problem can be expanded as

$$\begin{aligned} \phi_n(r) &= \phi_n^{(0)}(r) + \lambda\phi_n^{(1)}(r) + \lambda^2\phi_n^{(2)}(r) + \cdots; & (2.9)\\ (\omega_n)^2 &= (\omega_n^{(0)})^2 + \lambda(\omega_n^{(1)})^2 + \lambda^2(\omega_n^{(2)})^2 + \cdots. & (2.10)\end{aligned}$$

Then, to first order in λ,

$$n(r)a(r)b(r)\vec{q}^2\phi_n^{(0)}(r) + H^{(0)}(r)\phi_n^{(1)}(r) = \frac{a^3(r)b(r)}{n(r)}\left((\omega_n^{(1)})^2\phi_n^{(0)}(r) + (\omega_n^{(0)})^2\phi_n^{(1)}(r)\right) \tag{2.11}$$

We are looking for the first order correction $\Delta(\omega_n)^2 := (\omega_n^{(1)})^2$, therefore we take the inner product with $\phi_n^{(0)}(r)$. Due to the Hermiticity of $H^{(0)}(r)$, the last term on the left hand side cancels the last term on the right hand side. Note that Hermiticity is important here; one cannot take $\frac{n(r)}{a^3(r)b(r)}H^{(0)}(r)$ as the unperturbed operator because it is not Hermitian. The result is

$$\Delta(\omega_n)^2 = c_n^2\vec{q}^2, \tag{2.12}$$

where

$$c_n^2 := \frac{\int dr\, n(r)a(r)b(r)|\phi_n^{(0)}(r)|^2}{\int dr\, \frac{a^3(r)b(r)}{n(r)}|\phi_n^{(0)}(r)|^2}. \tag{2.13}$$

Finally, we see that the expected modified dispersion relation is

$$\omega_n^2 = M_n^2 + c_n^2 \vec{q}^{\,2} \tag{2.14}$$

and c_n is identified with the local maximal attainable speed of the n^{th} particle as seen on our brane.

If the wave function concentrates near the brane, it is justified to expand the expression for c_n^2 in a Taylor series about r_0, the position of the brane. In doing so, and keeping first order terms only, we get

$$c_n^2 = 1 + 2(n'(r_0) - a'(r_0)) \frac{\int dr\,(r - r_0)|\phi_n^{(0)}(r)|^2}{\int dr\,|\phi_n^{(0)}(r)|^2} + \mathcal{O}\left(\left[\frac{\int dr\,(r - r_0)|\phi_n^{(0)}(r)|^2}{\int dr\,|\phi_n^{(0)}(r)|^2}\right]^2\right) \tag{2.15}$$

This expansion shows that c_n^2 has small variations from 1 that depend on the shape of the wave function in the extra dimension. Note that we assumed the wave function to be narrow and concentrated near r_0. If that's not the case, then the expansion is not valid and greater changes to the form of c_n^2 are expected. Also, application of this method implies that the wave functions $\phi_n^{(0)}(r)$ of the unperturbed problem (2.8) (when $\vec{q} = 0$) are known. It is not obvious that one always knows them since the functions $n(r), a(r)$ and $b(r)$ can be complicated and later, we will perturb in the metric functions instead because we happen to know the solution in the unperturbed RS background. The reason why it was done this way in this subsection was to convince the reader that the dispersion relation gets modified for particles whose wave function extends in the extra dimension. It also has the advantage that it shows quite simply the main direction that this study intends to take which is to solve the problem as exactly as possible using numerical techniques. We worked on very general grounds in deriving our result by not specifying the metric functions. Next we describe the details of these functions, after which we will proceed to solve the problem with the other perturbation method before using numerical techniques.

2.2 Charged Black Hole Background

It was shown that the speed of a particle gets a dependence on the spread of its wave function in the bulk if the metric is asymmetric ($n(r) \neq a(r)$). Here, we wish to motivate such a background, and we will follow the treatment presented in [5].

The model for the 5D bosonic sector of the theory is as follows. We assume that the only sources in the bulk are a negative cosmological constant Λ_{bk}, a scalar field representing the graviton and a $U(1)$ gauge field. Then, the most general ansatz that keeps the homogeneity and isotropy of the spatial directions of the 3-brane, which we embed in this picture in the next section, is eq. (2.1), to which one could add time dependence to allow for expansion or contraction of the brane. The authors of [5] have shown that by using a 5D extension of Birkhoff's theorem[1], this ansatz can be reduced, by appropriate choice of coordinates, to

$$ds^2 := -h(r)dt^2 + \frac{r^2}{l^2}d\Sigma_{\tilde{k}}^2 + \frac{1}{h(r)}dr^2, \tag{2.16}$$

which is also the most general brane-universe solution [20]. One of the implications of Birkhoff's theorem is that from this choice of coordinates the background metric becomes static while the brane can generally still be moving [21], which describes an expanding universe. We will restrict ourselves to the stationary case for simplicity. Also note that this metric is of the form that represents a black hole located at $r = 0$. In this particular case where there is a $U(1)$ gauge field in the bulk, it is an AdS-Reissner-Nordström black hole. The metric function $h(r)$ which characterizes this spacetime is

$$h(r) := \tilde{k} + \frac{r^2}{l^2} - \frac{\mu}{r^2} + \frac{Q^2}{r^4}. \tag{2.17}$$

As said previously, we will only consider the $\tilde{k} = 0$ case. Other possibilities for $\tilde{k}$ are discussed in [5] where they are shown to be less interesting. This choice also makes the equations a little easier to solve. Here, l is the AdS length defined by $1/l^2 := -\kappa_5^2\Lambda_{bk}/6$, where $\kappa_5^2 = 8\pi G_5$ defines the 5D Planck scale. As r goes to infinity, the contributions from μ and Q become negligible and the metric asymptotes

[1] See [19] for an insightful proof and explanation of Birkhoff's theorem in the 4D case.

to the Anti-de Sitter spacetime, which is the name for a spacetime with a negative cosmological constant; that's why it is called an AdS-RN black hole. It is on scales larger than l that 4D gravity as we know it is recovered [4]. Without the $U(1)$ gauge field, there is one less integration constant, Q, and this would have been the AdS-Schwarzschild metric. The fact that we have this parameter allows us to evade the fine-tuning problem that plagues models that attempt to solve the cosmological constant problem. Here, Q adds the extra freedom that is necessary to make the 4D cosmological constant vanish on our brane without needing the brane tension to take a specific value[2]. In units where the 5D Planck scale is unity, the meaning of μ and Q is that they represent the (4+1) energy density and charge density of the black hole, respectively, and their value can be chosen to reproduce standard cosmology to arbitrary accuracy [23]. Note that for a Schwarzschild metric, one always has a horizon. For the RN black hole, there can be two, one or none, depending on the relation between the parameters. In section 2.4, we study this in more detail.

One may wonder how can a black hole exist in the bulk since it was assumed that particles were stuck to our brane. The answer, which was given in [24], is that there is graviton radiation leaving our brane. Eventually, this will create an arbitrarily high local energy density and form a black hole, without the need for a collapse of conventional matter to create it.

As a last note concerning the asymetrical spacetime, the reader may be interested to learn that such scenarios, although originally only inspired from the fundamental M-theory, actually have rigorous connections with it. This was studied in [25]. In particular, the interpretation of the AdS-RN black holes in the 10D spacetime context is that they are spinning D3-branes.

[2]Later, though, we will introduce a regulator brane to cut away the naked singularity. This has the effect of reintroducing fine-tuning, see [22] for example.

2.3 Embedding of a Brane in the Spacetime: $\mathbb{Z}_2$ Symmetry and Jump Conditions

In the previous section, a metric was found that presented the asymmetric warping that leads to a gravitational Lorentz violating effect. There are, however, a few features that must be added to the spacetime due to the presence of the brane.

Braneworlds with one extra dimension are usually inspired by a model derived from M-theory by Hořava and Witten [29, 30]. In this model, compactification on an orbifold construction requires the space to end at a boundary. One simple, elegant, and well-defined, way to implement this is to impose a $\mathbb{Z}_2$ symmetry that identifies points on either side of the orbifold fixed points. Since braneworlds are generally constructed in a similar fashion, with space ending on the brane, the $\mathbb{Z}_2$ symmetry of the metric about the brane is an equally good way to achieve this and is therefore commonly assumed. Although there have been some tentatives in describing braneworlds that break this symmetry (see for example [31]), the end result is that scenarios of this type must eventually revert to a $\mathbb{Z}_2$ symmetric form at late times to recover standard cosmology. For these reasons, throughout this work the tendency to stick with this symmetry is followed.

Explicitly, reference [32] shows how to construct braneworlds by gluing together two known solutions to Einstein's equations. The junction point of these solutions is interpreted as the brane. In the case where one takes two identical slices of spacetime, the $\mathbb{Z}_2$ symmetry is recovered[3]. Since the solution (2.16) asymptotes to the Randall-Sundrum AdS$_5$ solution at large r, we cut it near infinity, just as is done to get a finite 4D Planck scale, and replace it by a copy of the solution near the black hole. It is implemented as follows:

$$\text{for } r \leq r_0 \qquad ds^2 := -h(r)dt^2 + \frac{r^2}{l^2}d\Sigma_k^2 + \frac{1}{h(r)}dr^2; \tag{2.18}$$

$$\text{for } r \geq r_0 \qquad ds^2 := -h(r_0^2/r)dt^2 + \frac{r_0^4/r^2}{l^2}d\Sigma_k^2 + \frac{1}{h(r_0^2/r)}\frac{r_0^4}{r^4}dr^2, \tag{2.19}$$

where, as before, r_0 denotes the position of the brane.

[3] See [23] for another interesting view about how to construct $\mathbb{Z}_2$ symmetric braneworlds.

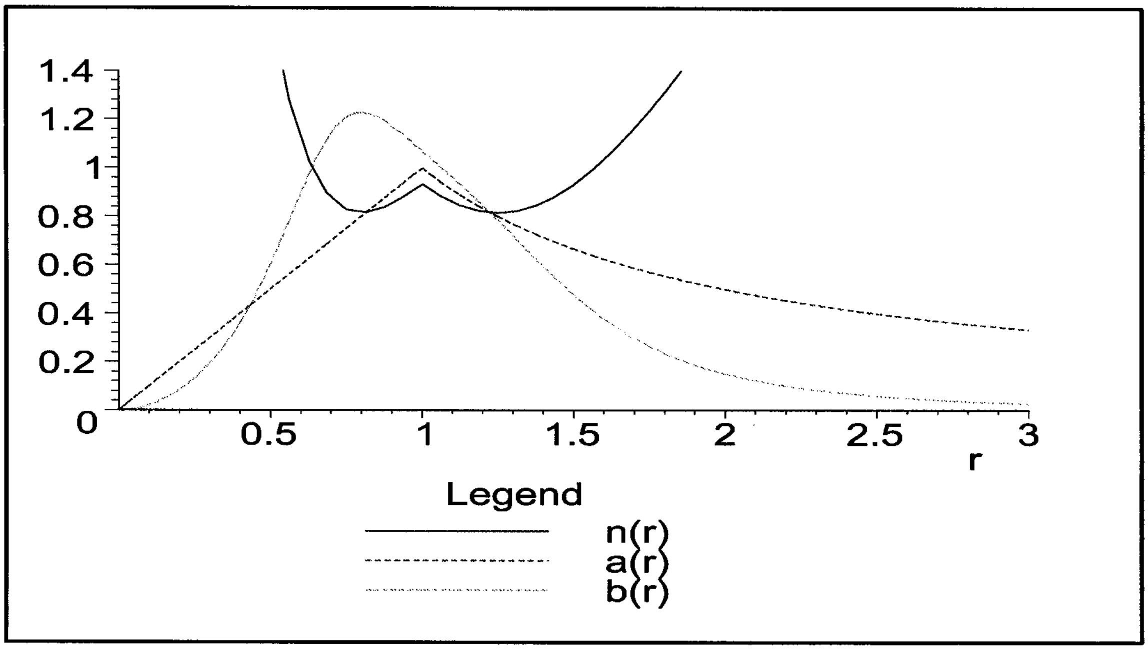

Figure 2.1: Plot of the metric functions (2.1) (here we have set $\mu = \frac{3}{2}\frac{Q^2}{r_0^2}, Q = 0.5, r_0 = l = 1$).

The metric functions are plotted in figure 2.1 in order to illustrate more clearly what is meant by the $\mathbb{Z}_2$ symmetry. For illustration purposes, we have set $r_0 = l = 1$, $\mu = \frac{3}{2}\frac{Q^2}{r_0^2}$ since this is the relation between the mass and charge of the black hole for an ordinary equation of state (see next section), and $Q = 0.5$. This value for Q was chosen only to show an appreciable deviation from the AdS_5 spacetime. Expressed with our radial coordinate r, it is seen that the symmetry exchanges the short and large distances, *i.e.* the long distance solution is a mirror of the short distance one through the relation $r \leftrightarrow r_0^2/r$. Notice that, due to the symmetry, there is a kink in the metric functions $a(r)$ and $n(r)$ at the position of the brane. In fact, for a metric of the general form (2.1), it was shown in [33] that for the geometry to be well defined, the following jump equations for the metric functions must be satisfied at the brane:

$$\frac{[a']}{a|b|} = -\frac{\kappa_5^2}{3}\rho, \tag{2.20}$$

$$\frac{[n']}{n|b|} = \frac{\kappa_5^2}{3}(2\rho + 3p), \tag{2.21}$$

where

ρ is the energy density of the brane and

p is the pressure.

The functions are evaluated at the brane's location in the extra dimension, and the notation $[f'] := f'(r^+) - f'(r^-)$ stands for the jump in the derivative of a function. These equations are obtained by requiring the metric to be continuous, but its first derivatives are allowed to be discontinuous (as is the case here) so that the resulting Dirac delta function in the second derivatives matches, through the 5D Einstein equations $G_{AB} = \kappa_5^2 T_{AB}$, the Dirac delta function in the stress-energy tensor $T^A_B|_{brane} = \frac{\delta(r-r_*)}{b}\mathrm{diag}(-\rho, p, p, p, 0)$ of an ideal infinitely thin brane (here ρ and p are constants with respect to position in the brane for a homogeneous cosmology). These jump conditions are exploited explicitly in the next section.

2.4 Physical Brane

Having found the conditions that the brane must satisfy in order to be correctly embedded in the spacetime, we now use them to define the range of permissible values of the parameters $(r_0, \rho_0, \tilde{\omega}_0)$ that describe a brane on which we put the standard model particles; we call it the physical brane. Here, $\tilde{\omega}_0 := \frac{p_0}{\rho_0}$ is the equation of state of the brane.

Using the jump equations (2.20-2.21), we deduce expressions for the mass and charge of the black hole in terms of the brane parameters. Recall the metric (2.18) from which we identify

$$\text{for } r \leq r_0 \qquad n := \sqrt{h(r)}, a := \frac{r}{l}, b := \frac{1}{\sqrt{h(r)}}; \tag{2.22}$$

$$\text{for } r \geq r_0 \qquad n := \sqrt{h(r_0^2/r)}, a := \frac{r_0^2}{lr}, b := \frac{1}{\sqrt{h(r_0^2/r)}}\frac{r_0^2}{r^2}; \tag{2.23}$$

(we could have taken the negative square root while doing this identification, but it amounts to the same thing because then the negative signs cancel since we have $\frac{[a']}{a|b|}$ and $\frac{[n']}{n|b|}$). Note that for n to be a well defined real quantity, we demand that $h(r) > 0$ for the part of the spacetime that we intend to keep, since then the t coordinate in the metric remains timelike and the r coordinate, spacelike. So in the following, we shall assume that the values of μ and Q are such as to make $h(r) > 0$; it is shown below that this is indeed the case. With these functions explicitly defined, and choosing to keep the interior region with the $r \leftrightarrow r_0^2/r$ $\mathbb{Z}_2$ symmetry understood as described previously, one gets $[a'] = -2/l$ and $[n'] = -h'/\sqrt{h}$. It then easily follows from (2.20) that

$$6\sqrt{h(r_0)} = \kappa_5^2 \rho_0 r_0, \tag{2.24}$$

from which it follows that $\rho_0 > 0$, the physical brane has a positive tension. At this stage, according to previous discussion, keeping the interior region is the natural thing to do if one wants a finite 4D Planck scale. In the next section, another possibility is discussed, where the exterior region is kept instead. Using (2.24) in (2.21) yields

$$18h'(r_0) = -\kappa_5^4(2 + 3\tilde{\omega}_0)\rho_0^2 r_0. \tag{2.25}$$

Substituting the expression $h(r) = \frac{r^2}{l^2} - \frac{\mu}{r^2} + \frac{Q^2}{r^4}$ in the square of (2.24), and in (2.25), we get

$$\begin{aligned} 36\left(\frac{r_0^2}{l^2} - \frac{\mu}{r_0^2} + \frac{Q^2}{r_0^4}\right) &= \kappa_5^4 \rho_0^2 r_0^2, &(2.26)\\ 36\left(\frac{r_0^2}{l^2} + \frac{\mu}{r_0^2} - 2\frac{Q^2}{r_0^4}\right) &= -\kappa_5^4(2 + 3\tilde{\omega}_0)\rho_0^2 r_0^2. &(2.27)\end{aligned}$$

Thus, as a consequence of the jump equations for a static brane (in the static case, the two equations are independent), the mass μ and charge Q of the black hole are related to the parameters of the physical brane, by

$$\hat{\mu} = 3\left(1 + \frac{1}{36}\tilde{\omega}_0 \hat{\rho}_0^2\right)\hat{r}_0^4, \tag{2.28}$$

$$\hat{Q}^2 = 2\left(1 + \frac{1}{72}(1 + 3\tilde{\omega}_0)\hat{\rho}_0^2\right)\hat{r}_0^6, \tag{2.29}$$

where, to simplify notation, we defined

$$\begin{aligned} \hat{r} &:= \frac{r}{l};\\ \hat{\rho}^2 &:= \kappa_5^4 l^2 \rho^2;\\ \hat{\mu} &:= \frac{\mu}{l^2};\\ \hat{Q}^2 &:= \frac{Q^2}{l^4}.\end{aligned}$$

That way, the hatted quantities are dimensionless and the distances are measured in units of l, the AdS_5 radius. These equations impose constraints on the brane parameters.

First, if $\hat{\rho}_0, \tilde{\omega}_0, \hat{\mu}$ and $\hat{Q}$ are physical fixed parameters, then the value of $\hat{r}_0$ is determined from (2.28-2.29), and a fine tuning corresponding to the cosmological constant problem is required. If, however, in a self-tuning approach, the values of $\hat{\mu}$ and $\hat{Q}$ are allowed to dynamically adjust themselves then it might be that any value of $\hat{r}_0$ is possible; one could position the physical brane anywhere in the extra dimension. This might be preferable since it could be positioned far from the black hole so that the space is closer to pure AdS_5, making it more natural to perturb in this background. But if $\hat{r}_0$ really is arbitrary, then a radion associated with it would be phenomenologically dangerous. For the moment, let us keep these considerations apart and leave $\hat{r}_0$ unspecified. It will be seen later, when the speed of gravity is computed, that there is actually no dependence of our result on the choice of $\hat{r}_0$.

Next, we would like to obtain some constraints on $\hat{\rho}_0$, apart from the $\hat{\rho}_0 > 0$ discussed above. From the positivity of $\hat{Q}^2$ it is deduced that

$$\hat{\rho}_0^2 \leq \frac{-72}{1+3\tilde{\omega}_0} \tag{2.30}$$

when $\tilde{\omega}_0 < -1/3$. This provides an upper bound on $\hat{\rho}_0$. When $\tilde{\omega}_0 > -1/3$, the inequality reverses, but that does not make sense as a lower bound because the requirement that $\hat{\rho}_0^2 \geq 0$ is already a stronger constraint.

Now, what about the brane equation of state, $\tilde{\omega}_0$? For a radiation gas, the equation is $\tilde{\omega} = 1/3$, for a non-relativistic gas, it is $\tilde{\omega} \approx 0$, but for the case of interest here, we choose $\tilde{\omega}_0 = -1$, which is the ordinary equation of state for a cosmological constant and represents pure brane tension. The restriction (2.30) then implies that $0 < \hat{\rho}_0 \leq 6$. Also, for that choice of equation of state, a nice relation between $\hat{\mu}$ and $\hat{Q}$ exists:

$$\hat{\mu} = \frac{3}{2}\frac{\hat{Q}^2}{\hat{r}_0^2}. \tag{2.31}$$

However, as Csáki, Erlich and Grojean showed in [5], there is no horizon hiding the black hole singularity for this particular value of $\tilde{\omega}_0$. This is generally thought of as

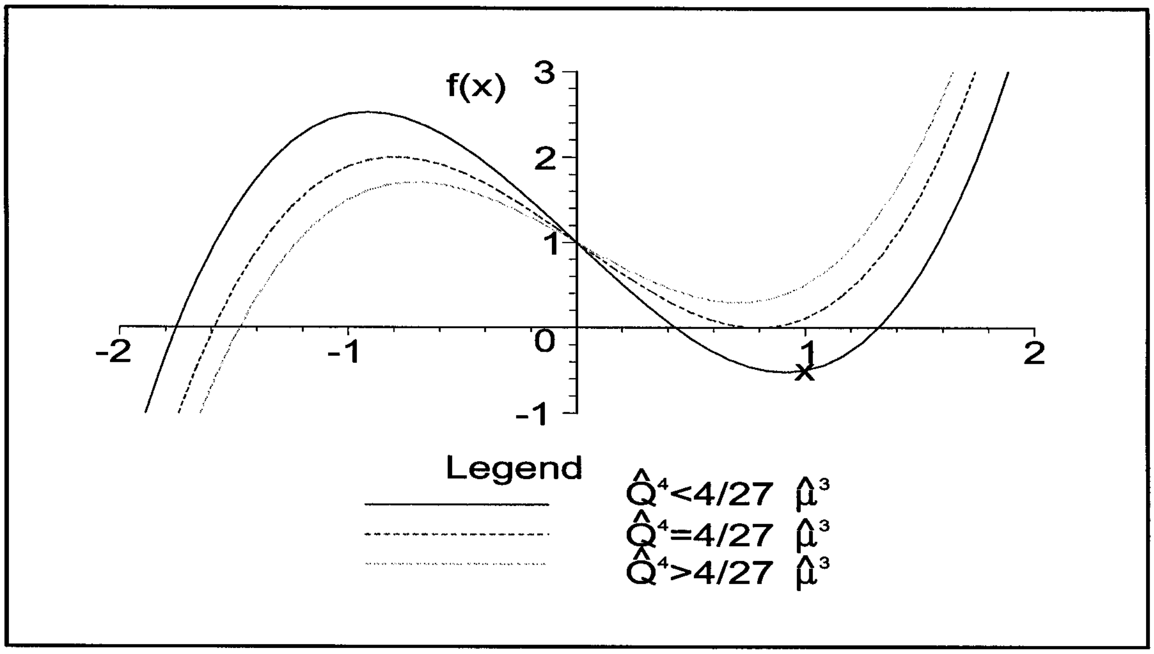

Figure 2.2: Plot of $f(x) = x^3/l^2 - \hat{\mu}x + \hat{Q}^2$. The positive roots, when present, show the position of the horizons. In these curves, $\hat{\mu}$ took the values 2.5, $(27/4)^{\frac{1}{3}}$ and 3/2, respectively, while $\hat{Q}$ was always equal to 1.

being unphysical since it violates the cosmic censorship conjecture [28]. It is seen that there is no horizon in our case in the following way. The horizon is the place where the $\hat{r}$ coordinate becomes timelike and the t coordinate, spacelike. Thus, at that point, $h(\hat{r}) = 0$, or equivalently, $\hat{r}^4 h(\hat{r}) = \hat{r}^6 - \hat{r}^2\hat{\mu} + \hat{Q}^2 = 0$. Letting $x := \hat{r}^2$, one looks for the positive roots of $f(x) := x^3 - \hat{\mu}x + \hat{Q}^2$. This is a polynomial of degree 3 with discriminant $4\hat{\mu}^3 - 27\hat{Q}^4$ (note that the discriminant is defined up to a sign). When this discriminant is positive, there are three unequal real roots; when it is zero, the roots are real with at least two of them equal; and when it is negative, there is only one real root. The behavior of $f(x)$ is shown in figure 2.2 for the different discriminants. Note that $f(0) = \hat{Q}^2$ and that $f'(0) = -\hat{\mu}$, which implies that there is always one and only one negative root (provided that $\hat{Q}^2 \neq 0$) since this is a degree 3 polynomial. So, if there are any remaining roots, then they must be positive, and of course, these are the interesting ones, associated with the horizons. If there are no positive roots, then there are no horizons. Thus, the condition for no horizon is that the discriminant be negative, or

$$\hat{Q}^4 > \frac{4}{27}\hat{\mu}^3. \tag{2.32}$$

Plugging the expressions for $\hat{\mu}$ (2.28) and $\hat{Q}^2$ (2.29), and rearranging some terms to make it easier to do the comparison, we get

$$\left(1 - \frac{1}{36}\hat{\rho}_0^2 + \frac{1}{24}(1+\tilde{\omega}_0)\hat{\rho}_0^2\right)^2 > \left(1 - \frac{1}{36}\hat{\rho}_0^2 + \frac{1}{36}(1+\tilde{\omega}_0)\hat{\rho}_0^2\right)^3. \tag{2.33}$$

With the choice $\tilde{\omega}_0 = -1$ for pure brane tension, this reduces to $0 > -\hat{\rho}_0^2$, which is clearly true, showing that there cannot be a horizon protecting from the black hole singularity and that $h(\hat{r}) > 0$ for every $\hat{r}$, as assumed previously. If $\tilde{\omega}_0$ was less than one, the story could change. The range of parameters that would permit the existence of horizons was studied in [5] but the end result is that this requires having exotic matter on the brane, which is not introduced here for simplicity[4]. We are left with a naked singularity that must be gotten rid of by cutting the spacetime with a second brane that we call the regulator brane.

2.5 Regulator Brane

Now that the acceptable values for the parameters of the physical brane are known, we seek those that are permissible for the regulator brane which is necessary to cut the spacetime before the naked singularity. So the problem of embedding this second 3-brane in the 5D black hole spacetime must be faced again. In the following, the parameters pertaining to the regulator brane are denoted by the subscript "-", because it is expected that it will be a negative tension brane. Luckily, most of the work was already done in the previous section; there are a few signs that must be treated carefully, however, before blindly replacing the subscripts "0" by the subscript "-". The jump equations (2.20) and (2.21) are derived on a very general basis and still apply, as is, for this second brane. The place where one has to be careful is in

[4]This is actually a general feature. In [27], the authors derive a no-go theorem for horizon-shielded self-tuning singularities which says in the case considered here that having self-tuning and a horizon requires violating the positive energy condition on the brane.

equations (2.18-2.19). The regulator brane must sit between the physical brane and the black hole if one decided to keep the interior space. Hence one keeps the exterior region with respect to the regulator brane. The inequalities in (2.18-2.19) then flip; consequently, $[a'] = +2/l$ and $[n'] = +h'/\sqrt{h}$. This then implies that (2.24) becomes

$$6\sqrt{h(r_-)} = -\kappa_5^2 \rho_- r_-; \tag{2.34}$$

unlike the physical brane, the regulator brane has a negative tension. Working out the second jump equation carefully, there are two sign changes which cancel each other and we get

$$18h'(r_-) = -\kappa_5^4(2 + 3\tilde{\omega}_-)\rho_-^2 r_-. \tag{2.35}$$

In solving for $\hat{\mu}$ and $\hat{Q}^2$, recall that (2.34) must be squared, which will cancel the newly introduced minus sign. So, although it is not obvious at first sight that the equations for $\hat{\mu}$ and $\hat{Q}^2$ should remain unchanged because the jump equations change sign at the regulator brane, they in fact still have the same form:

$$\hat{\mu} = 3\left(1 + \frac{1}{36}\tilde{\omega}_-\hat{\rho}_-^2\right)\hat{r}_-^4, \tag{2.36}$$

$$\hat{Q}^2 = 2\left(1 + \frac{1}{72}(1 + 3\tilde{\omega}_-)\hat{\rho}_-^2\right)\hat{r}_-^6. \tag{2.37}$$

Note that the motivation for keeping the interior region when placing the physical brane was that a horizon would naturally cut the space near the singularity. Having shown that this is not the case we introduced the regulator brane to play this role. But there is another way of cutting the space that provides a means for eliminating the naked singularity and a diverging 4D Planck scale. We could have taken the physical brane to be the inner brane and the regulator brane to be the outer one. The previous analysis shows that the sign flips cancel and we again have the same equations for $\hat{\mu}$ and $\hat{Q}^2$. The only thing that would change is that now the physical brane would have the negative tension while the regulator brane would have the positive one. This is an interesting option because then our scenario resembles the RS I model [3] and allows us to solve the hierarchy problem, *i.e.* the problem of why the electroweak scale ($M_{\rm EW} \approx 1$TeV) is so different from the Planck scale ($M_{\rm Pl} \approx 10^{16}$TeV) [17].

Their setup involves two branes, one with positive tension where the graviton is localized, and one with negative tension where the standard model particles (our world) are confined. The decreasing warp factor in their metric is what makes the gravitational coupling weaker on the negative tension brane and this generates an exponential hierarchy. In order to both follow the treatment of [5], which assumes that we live on the positive tension brane, and consider a solution to the hierarchy problem, we will not restrict ourselves to live on a particular brane. We will rather investigate the two cases, namely that the physical brane can be the positive or the negative tension one. A remark on the notation convention that will be assumed from now on: the "0" and "-" subscripts always refer to the positive and negative tension branes, respectively. The term "physical brane" refers to the brane on which we live, irrespective of the sign of its tension which varies depending on the situation that is considered; the "regulator brane" is the other one and has opposite tension.

Since $\hat{\mu}$ and $\hat{Q}^2$ are physical properties of the black hole, which are now fixed by the positive brane parameters, and are constants in the bulk, equations (2.36) and (2.37) are used in reverse to solve for $(\hat{r}_-, \hat{\rho}_-, \tilde{\omega}_-)$, the position, energy density and equation of state of the negative tension brane. By equating the expressions for $\hat{\mu}$ (2.28-2.36) and $\hat{Q}^2$ (2.29-2.37), we get

$$\left(1 + \frac{1}{36}\tilde{\omega}_0\hat{\rho}_0^2\right)\hat{r}_0^4 = \left(1 + \frac{1}{36}\tilde{\omega}_-\hat{\rho}_-^2\right)\hat{r}_-^4 \tag{2.38}$$

and

$$\left(1 + \frac{1}{72}(1 + 3\tilde{\omega}_0)\hat{\rho}_0^2\right)\hat{r}_0^6 = \left(1 + \frac{1}{72}(1 + 3\tilde{\omega}_-)\hat{\rho}_-^2\right)\hat{r}_-^6. \tag{2.39}$$

Since there are two equations and three unknowns, there is inevitably one parameter that must be specified. As a first attempt, specifying a valid equation of state for the negative brane seems easy and natural to do. But then, depending on the choice of $\tilde{\omega}_-$, there are times when it is possible to solve uniquely for the other two parameters $\hat{r}_-$ and $\hat{\rho}_-$, other times when there are two possible solutions and other times when there is no solution at all. So it appears that arbitrary values of $\tilde{\omega}_-$ are not permissible (the situation is described in detail in appendix A). This results in many difficulties that disappear when we change our point of view and decide to specify the value of $\hat{r}_-$ instead because this way of doing things allows us to choose the ratio

$$x := \frac{\hat{r}_-}{\hat{r}_0} \tag{2.40}$$

that solves the hierarchy problem.

Going back, then, to equations (2.38-2.39), $\tilde{\omega}_-$ is isolated in the former, plugged into the latter, and $\hat{\rho}_-^2$ is solved for. It is also easy to solve for $\tilde{\omega}_-$. With $\tilde{\omega}_0 = -1$, the results are

$$\hat{\rho}_-^2 = \hat{\rho}_-^2(x, \hat{\rho}_0, \tilde{\omega}_0 = -1) = 72\left[\left(1 - \frac{\hat{\rho}_0^2}{36}\right)\frac{1}{x^4}\left(\frac{1}{x^2} - \frac{3}{2}\right) + \frac{1}{2}\right] \tag{2.41}$$

and

$$\tilde{\omega}_- = \tilde{\omega}_-(x, \hat{\rho}_0, \tilde{\omega}_0 = -1) = \frac{\left(1 - \frac{\hat{\rho}_0^2}{36}\right)\frac{1}{x^4} - 1}{2\left(1 - \frac{\hat{\rho}_0^2}{36}\right)\frac{1}{x^4}\left(\frac{1}{x^2} - \frac{3}{2}\right) + 1}. \tag{2.42}$$

Plots of these functions are shown in figures 2.3 and 2.4. It is observed that, for $x < 1$ so that the negative tension brane is the inner one, as it should, the map between $\hat{\rho}_-^2$ and x is one-to-one. Also, there is no upper limit for $\hat{\rho}_-^2$, but there is a lower limit that is simply $\hat{\rho}_0^2$. Looking at the plot for $\tilde{\omega}_-$, now there is both a lower and an upper limit. The lower limit is -1 while the upper limit depends on $\hat{\rho}_0^2$. Furthermore, for $\tilde{\omega}_- > 0$, the plot is no longer one-to-one, which is the source of the difficulties mentioned earlier when $\tilde{\omega}_-$ was chosen as the specified parameter. This is why x is naturally a better choice.

It was mentioned that by choosing x, the hierarchy problem could be solved[5]. The appropriate value is $x \approx 10^{-16}$ [3], which means that $\hat{\rho}_0$ needs to be very close to 6 in order to generate a significant range for the $\hat{\rho}_-^2$ and $\tilde{\omega}_-$ parameters. Otherwise, $\hat{\rho}_-^2$ is incredibly large and $\tilde{\omega}_-$ is very nearly 0. Observe that it was the equation of state

[5]It is clear that this is true if we live on the negative tension brane since this is the Randall-Sundrum setup, but if we live on the positive tension brane this is less obvious. The authors of [35] suggest that this may still be possible if a warped supersymmetric extension of the model is introduced. We will not discuss the details of such a model, but just consider $x \approx 10^{-16}$ as an appropriate value for the inter-brane distance ratio in our two cases.

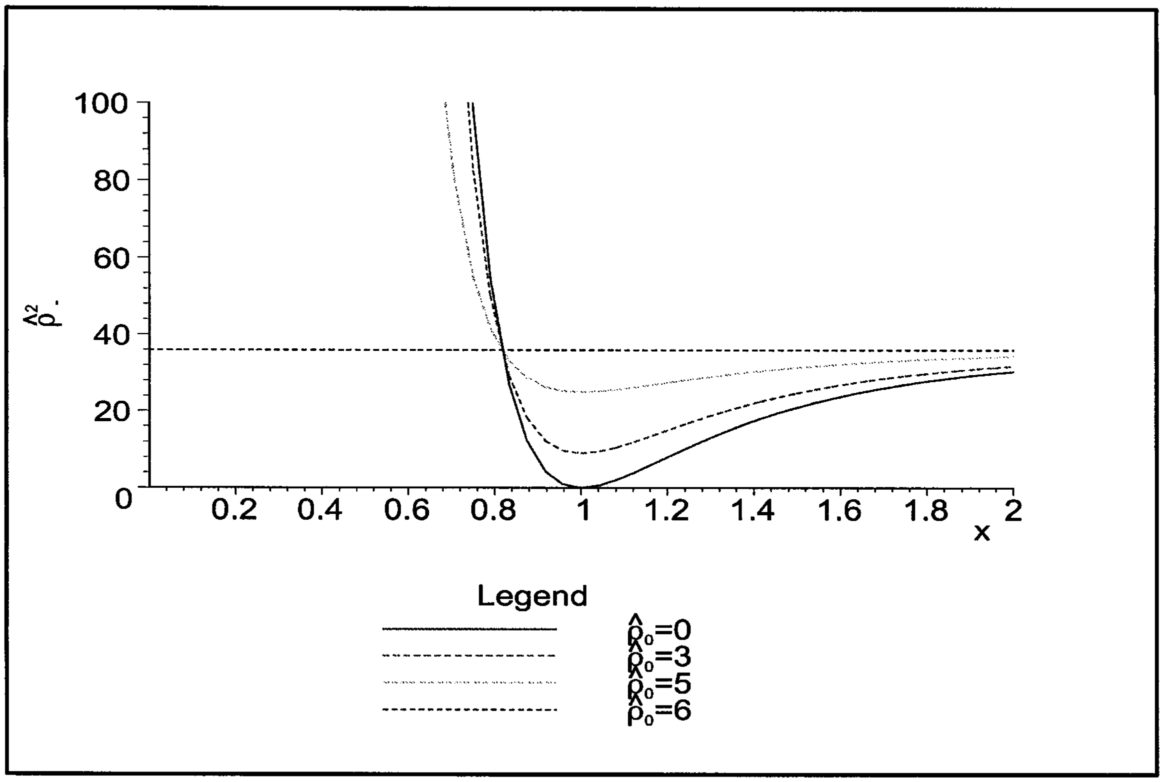

Figure 2.3: Energy density of the negative tension brane as function of its position (eq. (2.41)).

of the positive tension brane which was fixed. In the case where the physical brane is the negative one, $\tilde{\omega}_-$ could be slightly positive, depending on the value of $\hat{\rho}_0$. If we insist that the physical brane still has a -1 equation of state, then the $x > 1$ part of the graphs can be used to determine $\tilde{\omega}_0$. In the following, we concentrate on the $\tilde{\omega}_0 = -1$ case so that (2.31) holds. This will provide important simplifications later on.

2.6 RS Coordinates

Since we want to get the solution to the eigenvalue equation (2.5) by treating the metric (2.18-2.19) as a perturbation of the Randall-Sundrum background, it is logical to transform to the RS coordinates. The transformation is given explicitly by $\hat{r} \mapsto \hat{r}_0 e^{-ky}$, where $k := 1/l$, and the rescaling $(t, \vec{x}) \mapsto \frac{1}{\hat{r}_0}(t, \vec{x})$. Then, the metric becomes

$$ds^2 = -e^{-2k|y|}\hat{h}(y)dt^2 + e^{-2k|y|}d\vec{x}^2 + \frac{1}{\hat{h}(y)}dy^2 \tag{2.43}$$

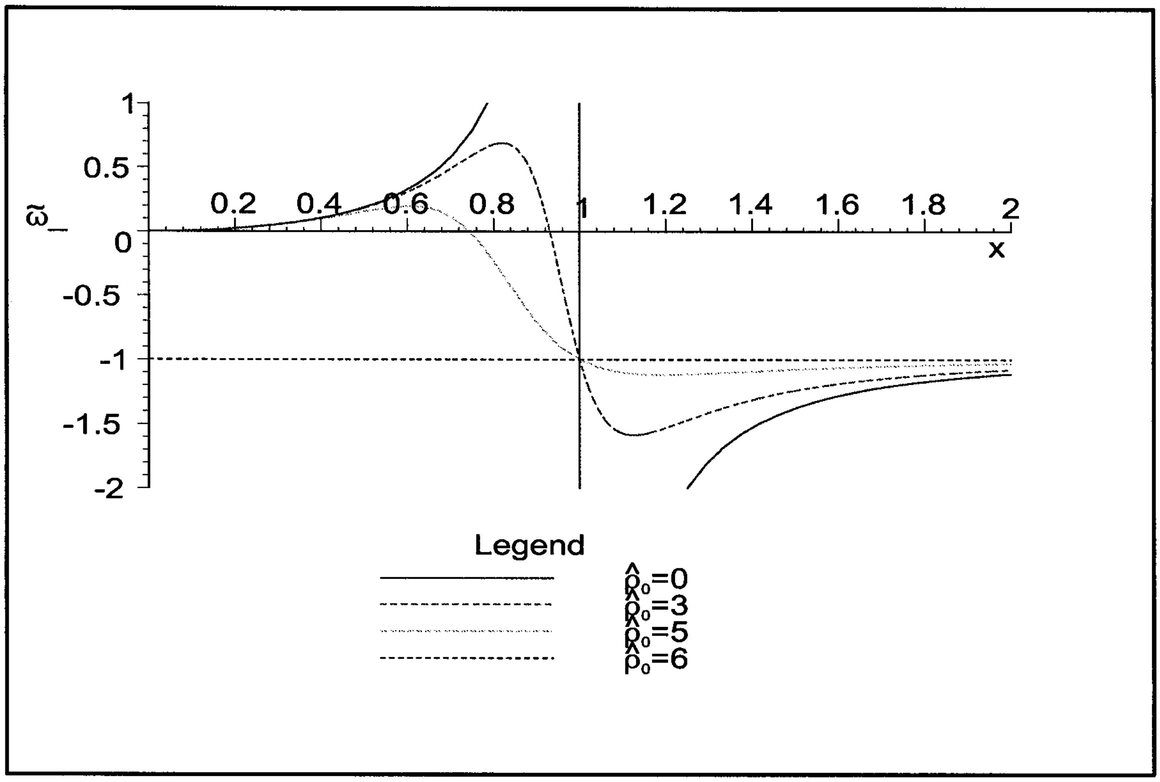

Figure 2.4: Equation of state of the negative tension brane as a function of its position (eq. (2.42)).

where now

$$y \qquad \text{is the extra dimension;} \tag{2.44}$$

$$\hat{h}(y) := 1 - \frac{\hat{\mu}}{\hat{r}_0^4} e^{4k|y|} + \frac{\hat{Q}^2}{\hat{r}_0^6} e^{6k|y|} \qquad \text{describes the black hole spacetime.} \tag{2.45}$$

The positive tension brane is at $y = 0$, the negative one at $y = y_-$ and the black hole is at infinity. Note that with these coordinates, the $\mathbb{Z}_2$ symmetry is taken care of by the absolute values of y; there is no more need for two different functions to describe the metric. This form for the metric is what will be used from now on. Observe further that, when there is no black hole ($\hat{\mu} = \hat{Q}^2 = 0$), the RS metric is recovered,

$$ds^2 = e^{-2k|y|} \left(-dt^2 + d\vec{x}^2\right) + dy^2. \tag{2.46}$$

This fact confirms that (2.43) has the appropriate form for perturbing in the RS background (see section 3).

Similarly, the equation of motion (2.5), becomes

$$\frac{a^3(y)b(y)}{n(y)}\omega^2\phi(y) = n(y)a(y)b(y)\vec{q}^2\phi(y) - \frac{1}{\hat{r}_0^2 e^{-2k|y|}}\partial_y\left(\frac{n(y)a^3(y)}{b(y)}\frac{1}{e^{-k|y|}}\partial_y\phi(y)\right) \tag{2.47}$$

for a metric of the form

$$ds^2 := -n^2(y)dt^2 + a^2(y)d\vec{x}^2 + \hat{r}_0^2 e^{-2k|y|}b^2(y)dy^2. \tag{2.48}$$

Comparing (2.43) and (2.48), one deduces

$$n(y) = e^{-k|y|}\sqrt{\hat{h}(y)}, \quad a(y) = e^{-k|y|}, \quad b(y) = \frac{1}{\hat{r}_0\sqrt{\hat{h}(y)}e^{-k|y|}} \tag{2.49}$$

for our case. Inserting these in (2.47), we get the final form for the equation of motion of a scalar field in the AdS-Reissner-Nordström metric:

$$\phi''(y) + \left(-4k\ \mathrm{sgn}(y) + \frac{\hat{h}'(y)}{\hat{h}(y)}\right)\phi'(y) + e^{2k|y|}\left(\frac{\omega^2}{\hat{h}^2(y)} - \frac{\vec{q}^2}{\hat{h}(y)}\right)\phi(y) = 0 \tag{2.50}$$

This is the equation we will seek to solve in the remaining parts of this work. It corresponds to the expansion of the equation for the propagation of a scalar in the background metric (2.43):

$$\Box\Phi = \frac{1}{\sqrt{|g|}}\partial_A(\sqrt{|g|}g^{AB}\partial_B\Phi) \equiv 0. \tag{2.51}$$

The boundary conditions, imposed by the $\mathbb{Z}_2$ symmetry, that ensure the evenness and smoothness of the solution at the orbifold fixed points are explicitly given by

$$\phi'(y)\big|_{y=0,y_-} = 0, \tag{2.52}$$

and the position of the negative brane appropriate for solving the hierarchy problem is given by $ky_- \approx 10\pi$.

3

Perturbative Approach

We mentioned that Csáki, Erlich and Grojean considered the black hole metric as a linearized perturbation around the RS spacetime. This calculation, which is repeated here for completeness, contrasts with the perturbation method used in subsection 2.1 in that it is not the momentum which is perturbed, but the metric functions. As said previously, it is done in this way because the solution in the RS background is known.

For the purposes of using the perturbation technique, let us write the perturbation as

$$\hat{h}(y) = \hat{h}^{(0)}(y) + \lambda \hat{h}^{(1)}(y) \tag{3.1}$$

where equation (2.45) dictates that

$$\begin{aligned} \hat{h}^{(0)}(y) &:= 1, & (3.2) \\ \hat{h}^{(1)}(y) &:= -\frac{\hat{\mu}}{\hat{r}_0^4} e^{4k|y|} + \frac{\hat{Q}^2}{\hat{r}_0^6} e^{6k|y|}. & (3.3) \end{aligned}$$

The solution is then expected to be of the form

$$\begin{aligned} \phi_n(y) &= \phi_n^{(0)}(y) + \lambda \phi_n^{(1)}(y) + \lambda^2 \phi_n^{(2)}(y) + \cdots; & (3.4) \\ \omega_n &= \omega_n^{(0)} + \lambda \omega_n^{(1)} + \lambda^2 \omega_n^{(2)} + \cdots. & (3.5) \end{aligned}$$

We will first solve the unperturbed problem and then add the first order correction.

3.1 Unperturbed Case Solution: $\hat{\mu} = \hat{Q}^2 = 0$

The unperturbed problem is the case without the black hole ($\hat{\mu} = \hat{Q}^2 = 0 \Rightarrow \hat{h}(y) = 1, \hat{h}'(y) = 0$); the eigenvalue equation (2.50) is reduced to

$$\phi_n''^{(0)}(y) - 4k \,\mathrm{sgn}(y)\, \phi_n'^{(0)}(y) + m_n^2 e^{2k|y|} \phi_n^{(0)}(y) = 0, \tag{3.6}$$

where

$$m_n^2 := (\omega_n^{(0)})^2 - \vec{q}^{\,2}. \tag{3.7}$$

Recall that here we work in the RS background (2.46). Since this metric is symmetric, the t and $\vec{x}$ coordinates are treated on equal footing. It is then appropriate to define $m_n^2 := (\omega_n^{(0)})^2 - \vec{q}^{\,2}$ as the separation constant when the separation of variables is performed. This is not possible when working in an asymmetrical background as can be seen from the equation of motion (2.47) where there is a difference in the coefficients multiplying ω_n^2 and $\vec{q}^{\,2}$. This is clearly apparent in eq. (2.50) where the relationship between ω_n^2 and $\vec{q}^{\,2}$ is altered by a function of y. Note that a subscript n is introduced. This is to emphasize the fact that this is an eigenvalue equation and that there are many eigenvalues satisfying it. We will refer to these different eigenvalues as the different modes of the scalar field.

Further insight about the meaning of m_n^2 can be obtained by decomposing the 5D action, with $\Phi^{(0)}(t,\vec{x},y) = \sum_n \varphi_n(t,\vec{x})\phi_n^{(0)}(y) := \sum_n e^{i(\omega_n t - \vec{q}\cdot\vec{x})}\phi_n^{(0)}(y)$:

$$\begin{aligned}
S_{5D} &= \frac{1}{2}\int d^4x\, dy\, \sqrt{|g|}g^{AB}\partial_A\Phi^{(0)}(t,\vec{x},y)\partial_B\Phi^{(0)}(t,\vec{x},y) && (3.8)\\
&= \frac{1}{2}\sum_{nm}\left[\int d^4x\,\eta^{\mu\nu}\partial_\mu\varphi_n\partial_\nu\varphi_m \int dy\, e^{-2k|y|}\phi_n^{(0)}\phi_m^{(0)}\right. && (3.9)\\
&\quad \left. + \int d^4x\,\varphi_n\varphi_m \int dy\, e^{-4k|y|}\partial_y\phi_n^{(0)}\partial_y\phi_m^{(0)}\right], \quad \text{integrate by parts} &&\\
&= \frac{1}{2}\sum_{nm}\left[\int d^4x\,\eta^{\mu\nu}\partial_\mu\varphi_n\partial_\nu\varphi_m \int dy\, e^{-2k|y|}\phi_n^{(0)}\phi_m^{(0)}\right. && (3.10)\\
&\quad \left. - \int d^4x\,\varphi_n\varphi_m \int dy\, \phi_m^{(0)}\partial_y(e^{-4k|y|}\partial_y\phi_n^{(0)})\right], \quad \text{recall (3.6)} &&\\
&= \sum_{nm}\left[\frac{1}{2}\int d^4x\, \left(\eta^{\mu\nu}\partial_\mu\varphi_n\partial_\nu\varphi_m + m_n^2\varphi_n\varphi_m\right)\int dy\, e^{-2k|y|}\phi_n^{(0)}\phi_m^{(0)}\right]. && (3.11)
\end{aligned}$$

By demanding that the state be normalized in the y direction, *i.e.*

$$\int dy\, e^{-2k|y|}\phi_n^{(0)}(y)\phi_m^{(0)}(y) \equiv \delta_{nm}, \tag{3.12}$$

the 5D action reduces to a 4D action $S_{4D} = \frac{1}{2}\sum_n \int d^4x\, \left(\eta^{\mu\nu}\partial_\mu\varphi_n\partial_\nu\varphi_n + m_n^2\varphi_n\varphi_n\right)$. Therefore, the bulk field $\Phi(t,\vec{x},y)$ is seen, by a 4D observer, as an infinite tower of scalars $\varphi_n(t,\vec{x})$ with masses m_n, which are the eigenvalues of equation (3.6).

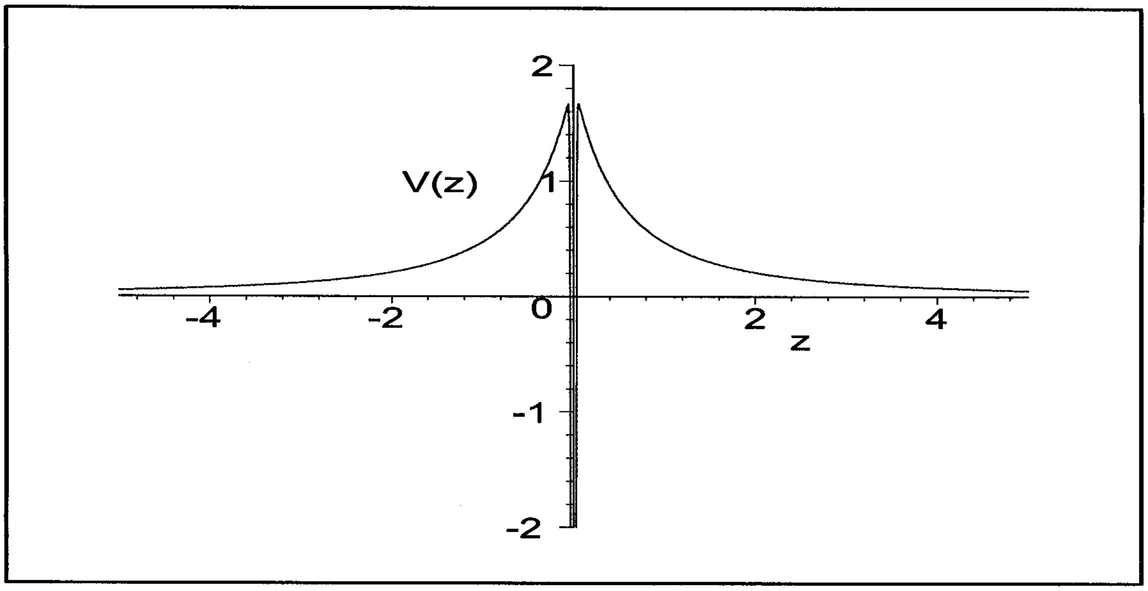

Figure 3.1: Quantum mechanics potential in the RS picture (eq. (3.14) with $k = 1$). There is one bound state due to the delta function at the position of the positive tension brane.

In [4], Randall and Sundrum transform the problem to a more familiar non-relativistic quantum mechanics one. Starting from (3.6) they change variables to $z := \mathrm{sgn}(y)(e^{k|y|} - 1)/k$ and $\hat{\psi}(z) := \frac{\phi_n^{(0)}(y)}{2} e^{-3k|y|/2}$, thus turning the problem into the Schrödinger equation, for which one has more intuition. They get

$$\left[-\frac{1}{2}\partial_z^2 + V(z)\right]\hat{\psi}(z) = \frac{m_n^2}{2}\hat{\psi}(z) \tag{3.13}$$

where the potential, sketched in figure (3.1), is

$$V(z) := \frac{15k^2}{8(k|z|+1)^2} - \frac{3k}{2(k|z|+1)}\delta(z). \tag{3.14}$$

From the shape of the potential, it is deduced that there is only one state bound to the positive tension brane because of the negative delta function. The bound state is the zero mass mode discussed in the next subsection. All other states are scattering states because the potential goes to zero at $\pm\infty$ and there is a continuum of Kaluza-Klein states with all possible $m_n^2 > 0$. This is modified by the presence of the negative brane which has the effect of quantizing the m_n's. Let us now derive those modes.

3.1.1 Zero Mode

For the zero mode ($m_0^2 = 0$), the solution to equation (3.6) is

$$\phi_0^{(0)}(y) = c_1 + c_2 \begin{cases} -\frac{e^{-4ky}}{4k} & \text{for } y \leq 0, \\ \frac{e^{4ky}}{4k} - \frac{1}{2k} & \text{for } y > 0. \end{cases} \tag{3.15}$$

Enforcing the boundary condition (2.52)

$$\phi_n'^{(0)}(y)\big|_{y=0} = 0, \tag{3.16}$$

we get that $c_2 = 0$. Thus, $\phi_0^{(0)}(y)$ is just a constant (this, incidentally, also satisfies the boundary condition at $y = y_-$).

Alternatively, the same result can be obtained by following the example in [36]. Letting $\psi_n(y) := e^{-2k|y|}\phi_n^{(0)}(y)$, the first derivative term disappears in (3.6) which becomes

$$[-\partial_y^2 - m_n^2 e^{2k|y|} + 4k^2 - 4k\delta(y)]\psi_n(y) = 0. \tag{3.17}$$

The difficulty arising from the presence of the delta function is that it makes the derivative of $\psi_n(y)$ discontinuous at $y = 0$ by the amount of $4k\,\psi_n(0)$, which we get by integrating the equation between $-\epsilon$ and ϵ, and taking the limit $\epsilon \to 0$. One must therefore be careful when matching the solutions for $y \leq 0$ and $y > 0$. In doing so for the zero mode, we obtain

$$\psi_0(y) = \begin{cases} c_3 e^{2ky} + c_4 e^{-2ky} & \text{for } y \leq 0, \\ -c_4 e^{2ky} + (c_3 + 2c_4)e^{-2ky} & \text{for } y > 0. \end{cases} \tag{3.18}$$

Demanding that the solution be finite for all y implies $c_4 = 0$, which yields $\psi_0(y) = c_3 e^{-2k|y|}$. Transforming back to the original function $\phi_0^{(0)}(y) = \psi_0(y)/e^{-2k|y|}$, it is again deduced that $\phi_0^{(0)}(y)$ is a constant. From the normalization condition (3.12) we get that

$$\phi_0^{(0)} = \sqrt{\frac{k}{1 - e^{-2ky_-}}} \overset{y_R \to \infty}{\longrightarrow} \sqrt{k}. \tag{3.19}$$

It may seem like the solution is not localized on the brane since it is a constant in the extra dimension. This would be undesirable if the scalar field is to represent the graviton responsible for our 4D gravity. The localization comes from the decreasing warp factor which effectively suppresses the wave function away from the positive tension brane.

3.1.2 Excited Modes

Next, we tackle the cases where $m_n^2 \neq 0$. We will refer to these as the excited modes and follow the reasoning described in [37]. As it turns out, eq. (3.17) is in fact Bessel's equation of order $\nu = 2$. To make this more obvious, momentarily change variables from y to $\zeta := \frac{m_n e^{k|y|}}{k}$; then eq. (3.6) can be recast, for $y \neq 0$, as

$$\zeta^2 \frac{d^2\psi_n(\zeta)}{d\zeta^2} + \zeta_n \frac{d\psi_n(\zeta)}{d\zeta} + (\zeta^2 - 4)\psi_n(\zeta) = 0, \tag{3.20}$$

which is one of the standard ways of writing Bessel's equation. The solutions to this equation are well known to be $J_2(\zeta)$ and $Y_2(\zeta)$, the second order Bessel functions of the first and second kinds, respectively. In terms of the original variables, the solution is

$$\phi_n^{(0)}(y) = \begin{cases} \frac{e^{2ky}}{N_n}\left(J_2\left(\frac{m_n e^{ky}}{k}\right) + b_n Y_2\left(\frac{m_n e^{ky}}{k}\right)\right) & \text{for } y > 0, \\ \frac{e^{-2ky}}{N_{n2}}\left(J_2\left(\frac{m_n e^{-ky}}{k}\right) + b_{n2} Y_2\left(\frac{m_n e^{-ky}}{k}\right)\right) & \text{for } y < 0. \end{cases} \tag{3.21}$$

where N_n, N_{n2}, b_n and b_{n2} are constants. As before the solutions must be matched at the brane: $\phi_n^{(0)}(y)|_{y=0-} = \phi_n^{(0)}(y)|_{y=0+}$, and $\phi_n'^{(0)}(y)\Big|_{y=0-} = \phi_n'^{(0)}(y)\Big|_{y=0+} = 0$. This permits to deduce that $N_n = N_{n2}$ and

$$\begin{aligned} b_n &= b_{n2} && (3.22)\\ &= \frac{2kJ_2\left(\frac{m_n}{k}\right) + m_n J_2'\left(\frac{m_n}{k}\right)}{2kY_2\left(\frac{m_n}{k}\right) + m_n Y_2'\left(\frac{m_n}{k}\right)} && (3.23)\\ &= -\frac{J_1\left(\frac{m_n}{k}\right)}{Y_1\left(\frac{m_n}{k}\right)}. && (3.24) \end{aligned}$$

The last equality follows from the derivative identity $\frac{d}{dx}[x^m J_m(x)] = x^m J_{m-1}(x)$ and a similar one for the function of the second kind. Putting that together, the full solution for the excited modes is written as:

$$\phi_n^{(0)}(y) = \frac{e^{2k|y|}}{N_n}\left(J_2\left(\frac{m_n e^{k|y|}}{k}\right) - \frac{J_1\left(\frac{m_n}{k}\right)}{Y_1\left(\frac{m_n}{k}\right)} Y_2\left(\frac{m_n e^{k|y|}}{k}\right)\right) \tag{3.25}$$

In the RS potential (3.14), this is not normalizable because the potential goes to zero; furthermore all masses are possible. But in our scenario, there is a black hole at infinity and a negative tension brane (and hence another delta function in the potential) is introduced to cut the space before the singularity. This has the consequence to quantize m_n. The boundary condition $\phi_n'^{(0)}(y)\Big|_{y=y_-} = \phi_n'^{(0)}(y)\Big|_{y=-y_-} = 0$ permits to find the eigenvalues m_n. We find

$$J_1\left(\frac{m_n}{k}e^{ky_-}\right) - \frac{J_1\left(\frac{m_n}{k}\right)}{Y_1\left(\frac{m_n}{k}\right)}Y_1\left(\frac{m_n}{k}e^{ky_-}\right) = 0, \tag{3.26}$$

or

$$J_1\left(x_n\right) - \frac{J_1\left(x_n e^{-ky_-}\right)}{Y_1\left(x_n e^{-ky_-}\right)}Y_1\left(x_n\right) = 0, \tag{3.27}$$

where

$$x_n := \frac{m_n}{k}e^{ky_-}. \tag{3.28}$$

It is not possible to isolate x_n in equation (3.27), so it must be solved numerically once y_- and k are specified. However, in the case where e^{ky_-} is known to be large, like in the solution to the hierarchy problem [3], where $ky_- \approx 10\pi$, then it can be approximated that $\frac{J_1\left(x_n e^{-ky_-}\right)}{Y_1\left(x_n e^{-ky_-}\right)} \approx 0$ and the above reduces to looking at the roots of the following function instead:

$$J_1\left(\frac{m_n}{k}e^{ky_-}\right) = 0. \tag{3.29}$$

By numerically evaluating the roots of the Bessel function, one concludes that

$$\begin{aligned} m_1/k &= 3.8317e^{-ky_-} && (3.30)\\ m_2/k &= 7.0156e^{-ky_-} && (3.31)\\ m_3/k &= 10.1735e^{-ky_-} && (3.32)\\ m_4/k &= 13.3237e^{-ky_-} && (3.33)\\ \vdots &= \vdots && \end{aligned}$$

For conventional matter on the positive tension brane, $k \sim M_{\mathrm{Pl}} \approx 10^{16}$ TeV [4]. This means that the mass splitting is of a few TeV; the excited states may be detected in future collider experiments. If matter is confined to the negative tension brane, then

$k \sim M_{\rm EW} \approx 1$ TeV. But m_n is the mass as seen on the brane at $y = 0$. Observers at $y = y_-$ will see a mass scaled by e^{ky_-} [17]. Therefore, the observed mass splitting is again of a few TeV.

On the other hand, if ky_- is close to 0, then the previous approximation cannot be used since equation (3.27) becomes a trivial identity. In this case, an exact numerical solution is needed. From now on, we will assume that e^{ky_-} is large and that the above approximation can be done. For the low lying modes then, $m_n/k \propto e^{-ky_-}$ is small, and so is $b_n = -\frac{J_1\left(\frac{m_n}{k}\right)}{Y_1\left(\frac{m_n}{k}\right)} \approx \frac{\pi}{4}\left(\frac{m_n}{k}\right)^2 \propto \frac{\pi}{4}e^{-2ky_-}$, as can be seen by using the asymptotic approximations of the Bessel functions. Thus, in this approximation, the Y_2 term can be neglected when integrating the solution. For example, it is now easier to normalize and find N_n:

$$\begin{aligned}
1 &\equiv \int_{-y_-}^{y_-} dy\, e^{-2k|y|}(\phi_n^{(0)}(y))^2 && (3.34)\\
&\approx \frac{2}{N_n^2}\int_0^{y_-} dy\, e^{2ky} J_2^2\left(\frac{m_n}{k}e^{ky}\right), \quad \text{because of the smallness of } b_n; && (3.35)\\
&= \frac{2}{N_n^2 k}\int_1^{e^{ky_-}} dt\, t J_2^2\left(\frac{m_n}{k}t\right) && (3.36)\\
&\approx \frac{2}{N_n^2 k}\int_0^{e^{ky_-}} dt\, t J_2^2\left(\frac{m_n}{k}t\right), \quad \text{the integral over } [0,1[\text{ is negligible;} && (3.37)\\
&= \frac{2}{N_n^2}\frac{e^{2ky_-}}{2k}\left[J_2^2\left(\frac{m_n}{k}e^{ky_-}\right) - J_1\left(\frac{m_n}{k}e^{ky_-}\right) J_3\left(\frac{m_n}{k}e^{ky_-}\right)\right] && (3.38)\\
&= \frac{e^{2ky_-}}{N_n^2 k} J_2^2\left(\frac{m_n}{k}e^{ky_-}\right), \quad \text{because of (3.29).} && (3.39)
\end{aligned}$$

Finally,

$$\phi_n^{(0)}(y) \approx \frac{e^{2k|y|}}{\frac{e^{ky_-}}{\sqrt{k}} J_2\left(\frac{m_n}{k}e^{ky_-}\right)} \left(J_2\left(\frac{m_n e^{k|y|}}{k}\right) + \frac{\pi}{4}\left(\frac{m_n}{k}\right)^2 Y_2\left(\frac{m_n e^{k|y|}}{k}\right)\right). \tag{3.40}$$

Of course, the zero mode solution that was obtained earlier can be derived from a limiting procedure. However, the normalization that was just found cannot be used. This is because that result was obtained by assuming that the Y_2 term could be omitted when doing the integral, but that is no longer true when $m_n \to m_0 = 0$. It is then better to proceed as follows:

$$\phi_n^{(0)}(y) \approx \frac{e^{2k|y|}}{N_n}\left(J_2\left(\frac{m_n e^{k|y|}}{k}\right) + \frac{\pi}{4}\left(\frac{m_n}{k}\right)^2 Y_2\left(\frac{m_n e^{k|y|}}{k}\right)\right) \tag{3.41}$$

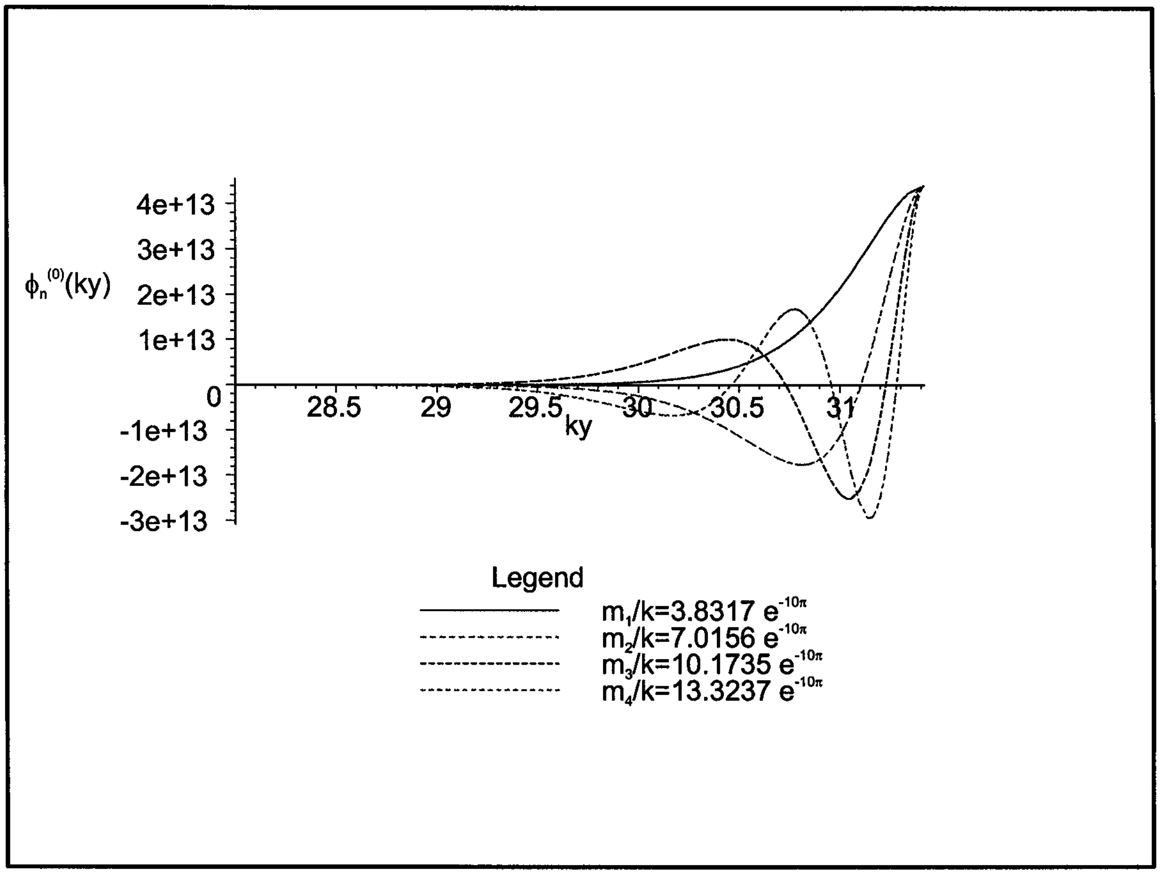

Figure 3.2: Wave functions for the first few excited modes (eq. (3.40)). $ky_- = 10\pi$ was used and only the region where there are interesting fluctuations are displayed.

$$\rightarrow \frac{e^{2k|y|}}{N_n}\left(\frac{1}{2}\left(\frac{m_n e^{k|y|}}{2k}\right)^2 + \frac{\pi}{4}\left(\frac{m_n}{k}\right)^2\left(-\frac{1}{\pi}\left(\frac{2k}{m_n e^{k|y|}}\right)^2\right)\right) \tag{3.42}$$

$$\rightarrow -\frac{1}{N_n}, \tag{3.43}$$

which is the same result as before, namely that $\phi_0^{(0)}$ is a constant. The correct normalization has already been done in the previous section.

In order to get a feel for the mathematical work that was done, the solutions are plotted in figure 3.2 for the low lying modes. The zero mode is not displayed because it is just a constant, too small compared to the other modes in this region. The main feature is that the excited modes are concentrated at the negative brane. They grow exponentially and they oscillate because of the Bessel functions.

3.2 Perturbed Case: $\hat{\mu}, \hat{Q}^2 \neq 0$

Just as in subsection 2.1 we now introduce a small perturbation. In this case it is $\lambda \hat{h}^{(1)}(y)$, the black hole of our scenario. The small correction terms $\phi_n^{(1)}(y)$ and $\omega_n^{(1)}$ are then expected to be proportional to the perturbation terms $\frac{\hat{\mu}}{\hat{r}_0^4} e^{4k|y|}$ and $\frac{\hat{Q}^2}{\hat{r}_0^6} e^{6k|y|}$ if these remain small in the interval between the branes. Note that this implies taking $\hat{\rho}_0$ very close to 6 to make $\hat{\mu}/\hat{r}_0^4$ and $\hat{Q}^2/\hat{r}_0^6$ sufficiently small, since we said that $ky_- \approx 10\pi$ (more on this in section 4). Our main concern here will be to find the correction term $\omega_n^{(1)}$ to the energy, without being overly concerned about the exact form of the corrected wave function.

3.2.1 Perturbative Zero Mode

Substituting (3.4-3.5) into the equation of motion (2.50) and keeping terms up to order λ only, and recalling that $(\omega_0^{(0)})^2 = q^2$ and that $\phi_0^{(0)}(y)$ is a constant for the zero mode, we get

$$\begin{aligned} \phi_0''^{(1)}(y) - 4k\,\mathrm{sgn}(y)\phi_0'^{(1)}(y) &= e^{2k|y|}\left(-2q\omega_0^{(1)} + q^2\hat{h}^{(1)}(y)\right)\phi_0^{(0)} && (3.44) \\ &= e^{2k|y|}\left(-2q\omega_0^{(1)} + q^2\left(-\frac{\hat{\mu}}{\hat{r}_0^4}e^{4k|y|} + \frac{\hat{Q}^2}{\hat{r}_0^6}e^{6k|y|}\right)\right)\phi_0^{(0)}. && (3.45) \end{aligned}$$

The left-hand side of this equation is linear and the inhomogeneous part contains only exponential functions of y. The method of undetermined coefficients can therefore be used to solve this differential equation. The general solution is

$$\phi_0^{(1)}(y) = \left(c_1 + c_2 e^{4ky} - \frac{1}{12}\frac{\hat{\mu}}{\hat{r}_0^4}\frac{q^2}{k^2}e^{6ky} + \frac{1}{32}\frac{\hat{Q}^2}{\hat{r}_0^6}\frac{q^2}{k^2}e^{8ky} + \frac{1}{2}\frac{\omega_0^{(1)}q}{k^2}e^{2ky}\right)\phi_0^{(0)}, \quad (3.46)$$

for $y > 0$. The boundary conditions $\phi_0'^{(1)}(y)\Big|_{y=0,y_-} = 0$, coming directly from eq. (2.52), permit to solve for c_2,

$$c_2 = \frac{1}{8}\frac{\hat{\mu}}{\hat{r}_0^4}\frac{q^2}{k^2}(1 + e^{2ky_-}) - \frac{1}{16}\frac{\hat{Q}^2}{\hat{r}_0^6}\frac{q^2}{k^2}(1 + e^{2ky_-} + e^{4ky_-}), \quad (3.47)$$

and to get an expression for the dispersion relation of the zero mode:

$$\omega_0^{(1)} = \frac{1}{4}q\left(-2\frac{\hat{\mu}}{\hat{r}_0^4} + \frac{\hat{Q}^2}{\hat{r}_0^6}(1 + e^{2ky_-})\right)e^{2ky_-}. \quad (3.48)$$

Since the unperturbed solution is to be recovered when the perturbation terms vanish it is deduced that $c_1 = 0$ because c_2 and $\omega_0^{(1)} \to 0$ as $\hat{\mu}$, $\hat{Q}^2 \to 0$.

Now, the linear dependence of $\omega_0^{(1)}$ on the momentum q implies that the velocity of the zero mode is

$$v_{\text{grav}_0} := \frac{\partial \omega_0}{\partial q} \tag{3.49}$$

$$\approx \frac{\partial(\omega_0^{(0)} + \omega_0^{(1)})}{\partial q} \tag{3.50}$$

$$= 1 + \left(-\frac{\hat{\mu}}{2\hat{r}_0^4} + \frac{\hat{Q}^2}{4\hat{r}_0^6}(1 + e^{2ky_-}) \right) e^{2ky_-} = \text{const.} \tag{3.51}$$

Here, v_{grav_0} is independent of momentum and thus the limiting speed is simply

$$c_{\text{grav}_0} := \lim_{q \to \infty} v_{\text{grav}_0} \tag{3.52}$$

$$= v_{\text{grav}_0}. \tag{3.53}$$

Since electromagnetic radiation is stuck on the physical brane located at y_{phys} and follows a null curve $ds^2 \equiv 0$, its speed of propagation is

$$c_{\text{em}} = \sqrt{\left(\frac{d\vec{x}}{dt}\right)^2} \tag{3.54}$$

$$= \sqrt{\hat{h}(y = y_{\text{phys}})}. \tag{3.55}$$

When the physical brane is the positive tension one ($y_{\text{phys}} = 0$), this is

$$c_{\text{em}} \approx 1 - \frac{\hat{\mu}}{2\hat{r}_0^4} + \frac{\hat{Q}^2}{2\hat{r}_0^6}. \tag{3.56}$$

If the jump equations (2.31), fixing the mass and the charge of the black hole, are used to relate $\hat{\mu}$ and $\hat{Q}^2$, the difference between the speed of the graviton zero mode and the speed of the photon in this background can be expressed as

$$(v_{\text{grav}_0} - c_{\text{em}})_{\text{perturbatively}} = (\cosh(2ky_-) - 1) e^{2ky_-} \frac{\hat{Q}^2}{2\hat{r}_0^6} \tag{3.57}$$

$$= \text{const. wrt } q \text{ to first order in } \hat{\mu} \text{ and } \hat{Q}^2 \tag{3.58}$$

$$\geq 0, \text{ always.} \tag{3.59}$$

So the perturbation approach of Csáki, Erlich and Grojean predicts that gravity will always propagate faster than light in such a spacetime.

If, on the other hand, we choose $y_{\text{phys}} = y_-$, then the results are

$$c_{\text{em}} \approx 1 - \frac{\hat{\mu}}{2\hat{r}_0^4} e^{4ky_-} + \frac{\hat{Q}^2}{2\hat{r}_0^6} e^{6ky_-}. \tag{3.60}$$

and

$$\begin{aligned}
(v_{\text{grav}_0} - c_{\text{em}})_{\text{perturbatively}} &= -(\cosh(2ky_-) - 1) e^{4ky_-} \frac{\hat{Q}^2}{\hat{r}_0^6} && (3.61)\\
&= \text{const. wrt } q \text{ to first order in } \hat{\mu} \text{ and } \hat{Q}^2 && (3.62)\\
&\leq 0, \text{ always.} && (3.63)
\end{aligned}$$

In opposition with the previous case, the speed of gravity is found to be slower than that of light on the negative tension brane.

3.2.2 Attempt at Finding a Perturbative Solution for the Excited States

Here, we try to extend the results from the previous section to the excited states. The motivation for knowing the propagation speeds of these modes is that Lorentz violating kinematics could influence the decays of such particles [15] and provide new signatures for the presence of extra dimensions. Proceeding similarly as before, but using (3.7) instead, we end up with the following differential equation for the correction function:

$$\begin{aligned}
\phi_n''^{(1)}(y) &- 4k\,\text{sgn}(y)\phi_n'^{(1)}(y) + e^{2k|y|} m_n^2 \phi_n^{(1)}(y) && (3.64)\\
&= -\hat{h}'^{(1)}(y)\phi_n'^{(0)}(y) - e^{2k|y|}\left(-(2m_n^2 + q^2)\hat{h}^{(1)}(y) + 2\sqrt{m_n^2 + q^2}\,\omega_n^{(1)}\right)\phi_n^{(0)}(y) && \\
& && (3.65)\\
&= 4k\frac{e^{4k|y|}}{\hat{r}_0^4}\left(\hat{\mu} - \frac{3}{2}\frac{\hat{Q}^2 e^{2k|y|}}{\hat{r}_0^2}\right)\phi_n'^{(0)}(y)\,\text{sgn}(y) && (3.66)\\
&\quad -e^{2k|y|}\left((2m_n^2 + q^2)\left(\hat{\mu} - \frac{\hat{Q}^2 e^{2k|y|}}{\hat{r}_0^2}\right)\frac{e^{4k|y|}}{\hat{r}_0^4} + 2\sqrt{m_n^2 + q^2}\,\omega_n^{(1)}\right)\phi_n^{(0)}(y). &&
\end{aligned}$$

The homogeneous equation is the Bessel equation, which has already been met. But that equation is not linear! Therefore, the method of undetermined coefficients is inapplicable. That makes the inhomogeneous equation much harder to solve. The method of variation of parameters could be an option, but the inhomogeneous part being so complicated, it is discouraging even to think about trying this method. In fact, inputing this equation in a symbolic mathematical software results in a long, unusable, solution with unperformed integrals. After considering many possible analytic approximations, we found that none were really suitable. Because of the difficulties involved in extending the perturbative technique used in [5], we try another method, one that is closer to the treatment used in section 2.1.

Restarting from (2.50) and redoing the change of variables $\psi_n(y) := e^{-2k|y|}\phi_n^{(0)}(y)$, the equation of motion is rewritten as

$$H\psi_n(y) = -\frac{\omega_n^2 e^{2k|y|}}{\hat{h}(y)}\psi_n(y), \tag{3.67}$$

where

$$\begin{aligned} H &:= \partial_y(\hat{h}(y)\partial_y) - 4k^2\hat{h}(y) + 2k\,\mathrm{sgn}(y)\,\hat{h}'(y) - q^2 e^{2k|y|} + 4k\hat{h}(y)\delta(y) && (3.68)\\ &= [\partial_y(\hat{h}^{(0)}\partial_y) - 4k^2\hat{h}^{(0)} + 2k\,\mathrm{sgn}(y)\,\hat{h}'^{(0)} - q^2 e^{2k|y|} + 4k\hat{h}^{(0)}\delta(y)] \\ &\quad +\lambda[\partial_y(\hat{h}^{(1)}\partial_y) - 4k^2\hat{h}^{(1)} + 2k\,\mathrm{sgn}(y)\,\hat{h}'^{(1)} + 4k\hat{h}^{(1)}\delta(y)] && (3.69)\\ &=: H^{(0)} + \lambda H^{(1)}, && (3.70) \end{aligned}$$

to first order in λ.

Note that $H^{(0)}$ is a Hermitian operator in the usual sense. This may not be obvious since the wave function does not vanish at the branes, and so the boundary terms that arise when integrating by parts in order to prove the Hermicity do not disappear. But here the periodicity of the space is what saves us. Explicitly, doing it only for the first term of $H^{(0)}$ which is the only one that is suspicious with regards to Hermicity, we get

$$\int_{-y_-}^{y_-} \psi_n^*\partial_y(\hat{h}^{(0)}\partial_y)\psi_m\,dy = \int_{-y_-}^{y_-} \partial_y(\psi_n^*\hat{h}^{(0)}\partial_y\psi_m) - \partial_y\psi_n^*\hat{h}^{(0)}\partial_y\psi_m\,dy \tag{3.71}$$

$$
\begin{aligned}
&= [\psi_n^* \hat{h}^{(0)} \partial_y \psi_m]_{-y_-}^{y_-} - \int_{-y_-}^{y_-} \partial_y \psi_n^* \hat{h}^{(0)} \partial_y \psi_m \, dy && (3.72) \\
&= [\psi_n^* \hat{h}^{(0)} \partial_y \psi_m]_{-y_-}^{y_-} \\
&\quad - \int_{-y_-}^{y_-} \partial_y (\partial_y \psi_n^* \hat{h}^{(0)} \psi_m) - \partial_y (\hat{h}^{(0)} \partial_y \psi_n^*) \psi_m \, dy && (3.73) \\
&= [\psi_n^* \hat{h}^{(0)} \partial_y \psi_m]_{-y_-}^{y_-} - [\partial_y \psi_n^* \hat{h}^{(0)} \psi_m]_{-y_-}^{y_-} \\
&\quad + \int_{-y_-}^{y_-} \partial_y (\hat{h}^{(0)} \partial_y \psi_n^*) \psi_m \, dy && (3.74) \\
&= \int_{-y_-}^{y_-} (\partial_y (\hat{h}^{(0)} \partial_y) \psi_n)^* \psi_m \, dy, && (3.75)
\end{aligned}
$$

where the boundary terms vanish because the functions at y_- are the same as those at $-y_-$.

Using this expansion for H and the previous expansions for ω_n and $\hat{h}(y)$, the unperturbed equation (3.17) can of course be recovered. The order λ equality is then

$$
H^{(1)} \psi_n^{(0)} + H^{(0)} \psi_n^{(1)} = -\frac{e^{2k|y|}}{\hat{h}^{(0)}} \left((\omega_n^{(0)})^2 \psi_n^{(1)} - (\omega_n^{(0)})^2 \frac{\hat{h}^{(1)}}{\hat{h}^{(0)}} \psi_n^{(0)} + 2\omega_n^{(0)} \omega_n^{(1)} \psi_n^{(0)} \right). \quad (3.76)
$$

Just as in section 2.1, we take the inner product with $\psi_n^{(0)}$ and use the Hermicity of $H^{(0)}$ to cancel the terms involving $\psi_n^{(1)}$. This yields

$$
\omega_n^{(1)} = \frac{-\langle \psi_n^{(0)} | H^{(1)} \psi_n^{(0)} \rangle + (\omega_n^{(0)})^2 \langle \psi_n^{(0)} | \frac{\hat{h}^{(1)}}{(\hat{h}^{(0)})^2} e^{2k|y|} \psi_n^{(0)} \rangle}{2\omega_n^{(0)} \langle \psi_n^{(0)} | \frac{e^{2k|y|}}{\hat{h}^{(0)}} \psi_n^{(0)} \rangle}. \quad (3.77)
$$

The inner product in the denominator is just 1, if we use the normalization (3.12). Putting in the explicit form of $H^{(1)}$, the expression becomes

$$
\begin{aligned}
\omega_n^{(1)} &= -\frac{1}{\omega_n^{(0)}} \int_0^{y_-} \psi_n^{*(0)} (\partial_y (\hat{h}^{(1)} \partial_y) - 4k^2 \hat{h}^{(1)} + 2k \hat{h}'^{(1)}) \psi_n^{(0)} \, dy \\
&\quad + \omega_n^{(0)} \int_0^{y_-} \psi_n^{*(0)} \frac{\hat{h}^{(1)}}{\hat{h}^{(0)}} e^{2ky} \psi_n^{(0)} \, dy && (3.78) \\
&=: -\frac{1}{\omega_n^{(0)}} A_n(\hat{h}) + \omega_n^{(0)} B_n(\hat{h}). && (3.79)
\end{aligned}
$$

Since $\omega_n^{(0)} = \sqrt{m_n^2 + q^2}$, and $m_n/k \propto e^{-ky_-}$, all the terms are roughly comparable for $q \ll m_n$. But, for large momentum q, only the second integral is important. In that case,

$$
\omega_n^{(1)} \approx q \int_0^{y_-} |\psi_n^{(0)}|^2 \frac{\hat{h}^{(1)}}{\hat{h}^{(0)}} e^{2ky} \, dy \quad (3.80)
$$

$$= q \int_0^{y_-} |\psi_n^{(0)}|^2 \left(-\frac{\hat{\mu}}{\hat{r}_0^4} e^{6ky} + \frac{\hat{Q}^2}{\hat{r}_0^6} e^{8ky} \right) dy \tag{3.81}$$

$$\approx \frac{q}{N_n^2} \int_0^{y_-} J_2^2 \left(\frac{m_n e^{ky}}{k} \right) \left(-\frac{\hat{\mu}}{\hat{r}_0^4} e^{6ky} + \frac{\hat{Q}^2}{\hat{r}_0^6} e^{8ky} \right) dy \tag{3.82}$$

The last approximation is the same that has been done before, *i.e.* we assume that the Y_2 term can be neglected when integrating. The resulting integral, although simplified compared with our original expression, can still not be performed analytically; the second term, and most important one, resists every attempt that was made. Even expanding the Bessel function in a Taylor series does not help, too many terms would have to be kept in order to mimic appropriately the behavior of the wave function near the regulator brane. This is rather disappointing since we are thus reduced to using numerical integration. However, our analysis is still useful in the sense that it tells us that the first correction term to ω_n is proportional to q for large enough momentum, just as for the zero mode, while it should be inversely proportional to this quantity for low momentum (if we can still assume that $q \gg m_n$). Moreover we can show how the dispersion relation is expected to change. Squaring eq. (3.5) results in

$$\omega_n^2 = (\omega_n^{(0)} + \lambda \omega_n^{(1)} + \cdots)^2 \tag{3.83}$$

$$\approx (m_n^2 + q^2)(1 + 2B_n(\hat{h})) - 2A_n(\hat{h}) \tag{3.84}$$

to first order in λ. Comparing with the usual dispersion relation (2.7), it is deduced that the limiting speed of the n^{th} mode has been modified to

$$c_{\text{grav}_n}^2 = 1 + 2B_n(\hat{h}) \tag{3.85}$$

and that the mass of the mode changes due to the presence of the black hole perturbation:

$$M_n^2 = m_n^2(1 + 2B_n(\hat{h})) - 2A_n(\hat{h}). \tag{3.86}$$

In terms of these, the group velocity of the n^{th} mode with momentum q is

$$v_{\text{grav}_n} := \frac{\partial \omega_n}{\partial q} \tag{3.87}$$

$$\approx \frac{c^2_{\mathrm{grav_n}} q}{\sqrt{M_n^2 + c^2_{\mathrm{grav_n}} q^2}}. \tag{3.88}$$

As a consistency check, it can be verified that this result reduces to the previous one for the zero mode case where it is possible to do the integrals. In fact, plugging $\psi_0^{(0)}(y) = \sqrt{\frac{k}{1-e^{-2ky_-}}} e^{-2ky}$ into (3.79), the first integral, $A_0(\hat{h})$, vanishes and the second one, $B_0(\hat{h})$, yields exactly the result (3.48) that was obtained from a different method. The speeds of gravity (3.51) and (3.85) then also agree. In this case the mode remains massless, $M_0 = 0$, to first order.

Since it is not really worth using numerical techniques to compute the integrals $A_n(\hat{h})$ and $B_n(\hat{h})$ just to get what will be an approximate result anyway, in the next section, we redo the calculation for the speed of gravity, but this time using numerical methods on the exact equation (2.50). That way we will be able to investigate not only small perturbations, but larger ones as well. We will observe the behavior of $v_{\mathrm{grav_n}} - v_{\mathrm{em}}$ for the zero mode and the first low-lying ones. In particular, we want to find out if the dispersion relation always remains linear at large q and if the speed difference could change sign.

4

Numerical Solution

After trying to extend the perturbative solution to the excited states and not being able to find an analytic form, we end up needing numerical techniques to solve our difficulties.

4.1 *Method*

Starting with equation (2.50) for the equation of motion of ϕ in the bulk, equation (2.31) is used to eliminate $\hat{\mu}$ in favor of $\hat{Q}^2$. Note that the way of writing the perturbation (2.45) is misleading in a sense because it gives the appearance that the equation is dependent on $\hat{r}_0$. Remembering equation (2.29) for $\hat{Q}^2$, however, the $\hat{r}_0^6$ dependence is seen to cancel out. The variables that the equation really depends on are then q, y and $\hat{\rho}_0$ (it would also depend on $\tilde{\omega}_0$, but it was already fixed to be -1). For ease of computation, let us further define $\delta := 36 - \hat{\rho}_0^2$, which is a measure of how close $\hat{\rho}_0$ is to 6. This allows to quantify the perturbation and thus to make comparisons with the perturbation approach which, may be recalled, is only valid when the perturbation terms $\frac{\hat{\mu}}{\hat{r}_0^4}e^{4k|y|}$ and $\frac{\hat{Q}^2}{\hat{r}_0^6}e^{6k|y|}$ remain small compared to 1 in the interval between the branes. In terms of δ, $\hat{Q}^2/\hat{r}_0^6 = \delta/18$ and the equation of motion is rewritten as

$$\phi''(y) - 4k\ \mathrm{sgn}(y)\left(\frac{1-\frac{\delta}{36}e^{6k|y|}}{\hat{h}(y)}\right)\phi'(y) + e^{2k|y|}\left(\frac{\omega^2}{\hat{h}^2(y)} - \frac{q^2}{\hat{h}(y)}\right)\phi(y) = 0, \tag{4.1}$$

where now

$$\hat{h}(y) = 1 + \frac{\delta}{18}e^{4k|y|}\left(-\frac{3}{2} + e^{2k|y|}\right). \tag{4.2}$$

The domain of small perturbations is then simply

$$\Delta := \frac{\delta}{18}e^{6ky_-} \ll 1, \tag{4.3}$$

where only the $\hat{Q}^2$ restriction was used because it is the strongest one. Δ is defined to be the value of the perturbation. For the case where $e^{ky_-} \approx 10^{16}$ to solve the hierarchy problem, this means that $\delta \ll 1.8 \times 10^{-95}$, which justifies the previous statement that $\hat{\rho}_0$ is very nearly equal to 6 [1]. For simplicity, we will let $k = 1$ to set the scale of the problem.

Our goal now is to solve numerically the boundary value problem defined by equation (4.1) with boundary conditions (2.52). **MAPLE**'s numeric routines were used; they proved to work better than the *Numerical Recipes*' shooting technique [38] for this situation. It is quite understandable that this problem is hard to solve since the equation contains great hierarchies due to the exponential functions of y and the smallness of δ (4.3). It may be thought that changing variables to the previous $\psi(y)$ would remove part of the hierarchy and make the equation easier to solve, but that turned out not to be the case; the computation times were even greater and convergence of the method less frequent. Computations for large values of y remain difficult to perform. We therefore concentrate on solving the problem correctly for small hierarchies and then try to extrapolate the results to greater ones.

Once a list of values for ω as a function of q and δ is obtained for a given mode, the extraction of its speed of propagation is done by numerically computing the derivative (3.87). To exhibit the difference between the speed of the graviton's n^{th} mode and that of an ordinary particle with the same mass, with usual maximum speed c_{em}, we plot

$$\frac{v_{\text{grav}_\text{n}} - v_{\text{em}}}{v_{\text{em}}}, \tag{4.4}$$

where v_{em} is simply the expression (3.88) with c_{em}, given by (3.55), in place of c_{grav}. This gives the factor by which the velocity is increased for gravitons with respect to ordinary particles stuck on our 3-brane. Note that, here, the numerical result ($M_n^2 = \omega^2$ when $q = 0$) is used for the mass of the particle in the expression for

[1] This may look like a fine-tuning, but it is not a real one. It is not a requirement that δ be that small for the solution to the hierarchy problem to work. This is merely a requirement to ensure that the perturbation method is valid.

v_{em}. It would not have been totally appropriate to use (3.86) in v_{em} because then the particles that are being compared may not have exactly the same mass. Still, the approximate mass is used in the computation of the first order prediction from perturbation theory.

4.2 Results

The results yielded by the numerical procedure described above are displayed in this section. We show that in the perturbative regime we recover the predicted behavior of section 3, but that this behavior changes for stronger perturbations.

4.2.1 Zero Mode

The zero mode case is perhaps the most important one because it is responsible for the $1/r^2$ behavior in Newton's law of gravity [4]. It is also the one for which the first order result in perturbation theory is most complete, with predictions for the energy, speed difference and wave function corrections. Recall that for this case, the unperturbed solution is simply a constant and that the first correction is given by (3.46). This is dominated by a term going like e^{8ky} and can therefore already be seen to yield unreasonable results at large y_-. This is verified by plotting both the perturbative solution and the numerical result for different values of y_- (figure 4.1). For the lower y_-, there is good agreement between the two solutions. However, starting at about $y_- \approx 4$ (this value actually depends on q and δ), the deviations between the two solutions are becoming important. Whereas the perturbative solution becomes increasingly negative, the numerical one flattens out to 0. The wave function is therefore no longer constant and feels the negative tension brane less and less as the distance between the branes is increased. The fact that the perturbative result is diverging from the true solution at higher y_- is important to note for the computation process because it is the first order result that is used for the first initial guess. As can be seen, this is not always appropriate and can result in longer computation times and nonconvergence. In those cases where the first order result is too far from the

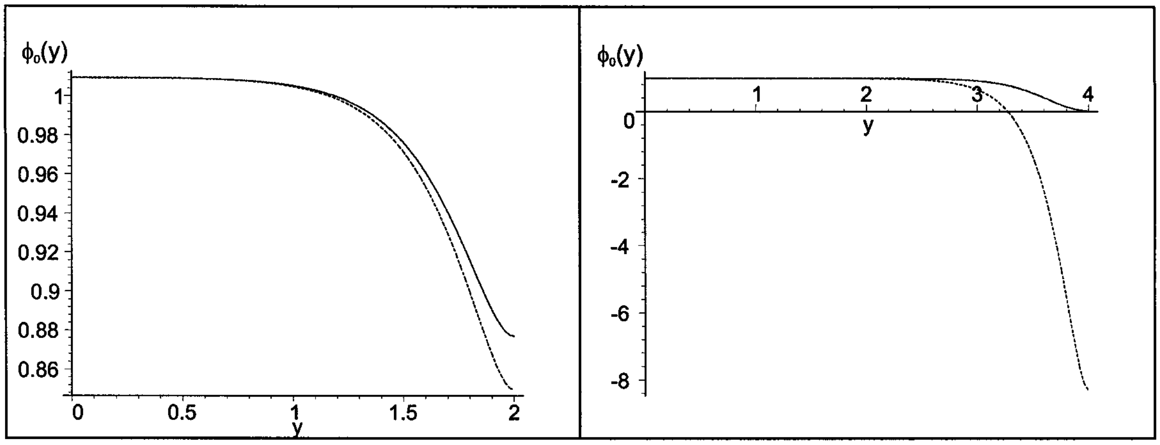

Figure 4.1: Zero mode wave function at different positions of the negative tension brane. The blue curve shows the first order prediction from perturbation theory and the red one shows the true (numerical) solution. The plot at the left is for $y_- = 2$ and that at the right is for $y_- = 4$; here $q = 1$ and $\Delta = .1$ for both plots.

exact one, it is best then just to use the unperturbed solution, which is actually closer to it.

Figure 4.2 shows the orthogonal projections of a three-dimensional plot of the correction to $\omega_0^{(0)}$ as a function of q and Δ. This allows us to verify the computation of the energy eigenvalue. As expected, the numerical and perturbative results are in better agreement for lower perturbations. What comes as a surprise though, is that there is also better agreement at low q, which was not believed to be a requirement for the small perturbation regime. It really is the appropriate combination of q and δ that makes the numerical and perturbative solutions agree. The higher the perturbation, the lower q needs to be, and vice versa. In the example shown, where Δ ranges from 0.1 to a value as high as 1, the results are in fair agreement, even for the large perturbation, provided that q is kept small (0.05 in this case). And a weak perturbation of $\Delta = 0.1$ can give an unacceptable first order result if q is large enough (not shown here since the graph stops at $q = 2$). This was found to be the case for even smaller perturbations.

At this point, one might wonder what is the value of ω_0 when $q = 0$, or equivalently, does the zero mode acquires a mass due to the perturbation? Although we were not able to compute directly with $q = 0$ for this particular mode, the tendency of

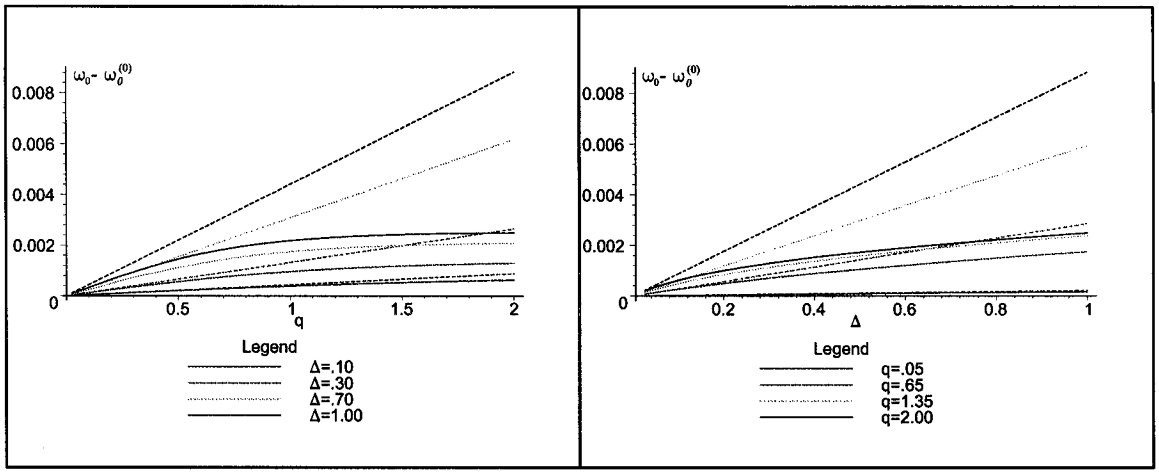

Figure 4.2: Correction to $\omega_0^{(0)}$ as a function of q and Δ. The dotted lines show the perturbative prediction (3.48), while the solid lines show the numerical result. Each color represents a different perturbation or momentum, and $y_- = 2$.

$\omega_0 - \omega_0^{(0)}$ to decrease with q indicates that the curve indeed passes through the origin. Furthermore, since the theory should reduce to 4D general relativity at low energies, and the graviton mass is forbidden by general covariance, there is good reason to believe that the mode remains massless as perturbation theory showed to first order.

With $M_0 = 0$, (4.4) is in fact $(v_{\text{grav}_0} - c_{\text{em}})/c_{\text{em}}$. This is plotted in figure 4.3, along with the perturbative prediction (3.57) for the case where the positive tension brane is the physical one. The first plot shows the dependence of the velocity on the momentum. As noted earlier, the perturbative approach does not show this dependence, hence the horizontal lines in the first graph and the unique dotted line in the second graph (displayed in red, but valid for all momenta). The numerical calculation shows on the contrary that the speed of the particle is q-dependent. Moreover, it is interesting to note that v_{grav_0} is decreasing monotonically with q instead of remaining constant, as is normally the case for a massless particle in our everyday world. It is also bounded from below. Therefore, c_{grav_0} as defined in (3.52) is not a limiting speed in the sense that it is the maximum speed, but rather a lower bound for the speed of gravity and that lower bound corresponds to c_{em} since the curves eventually all go to 0, no matter what the perturbation is. There is also an upper bound to v_{grav_0}, given by $q \to 0$ and it corresponds to the perturbative result for small perturbations,

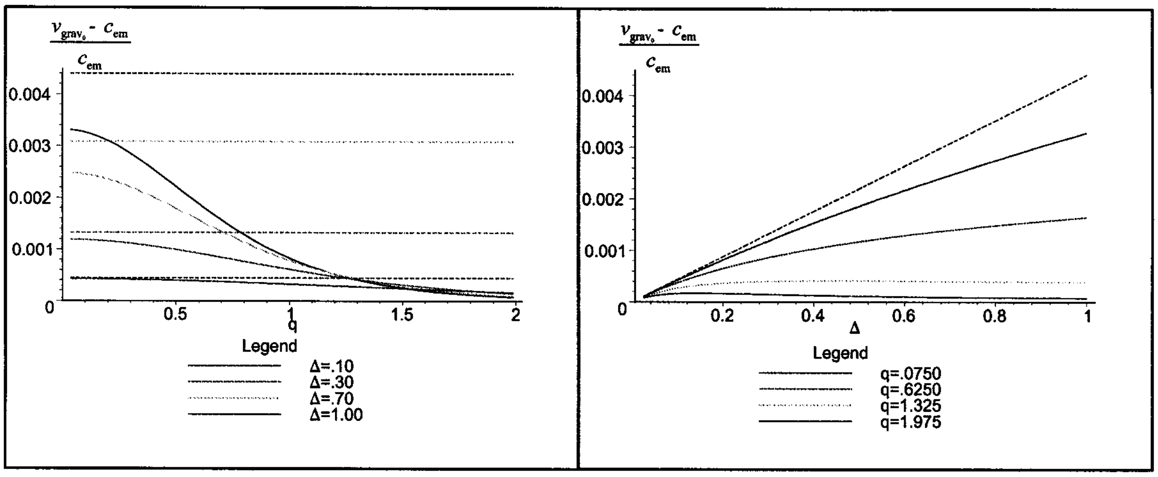

Figure 4.3: Relative speed difference between the gravity zero mode and the photon as a function of q and Δ when the physical brane has positive tension. The dotted lines show the perturbative prediction derived from (3.57), while the solid lines show the numerical result. Each color represents a different perturbation or momentum, and $y_- = 2$.

but is lower than this for Δ closer to 1. From these results, it is seen that the usual dispersion relation gets modified in a more complicated way than what was expected. It is not clear at this point what the correct form should look like, analytically. We can comment, though, that the reason why the effect disappears at high energies is that the de Broglie wavelength which is proportional to $1/q$ is becoming shorter than the AdS length l. Therefore, the energetic gravitons do not see the spacetime curvature, nor therefore the Lorentz invariance breaking, and they propagate as in flat space, bending negligibly in the bulk. Hence the speeds of propagation tend to the conventional value. The second plot shows the dependence on the magnitude of the perturbation. For small Δ, the behavior is linear, as expected, but for larger perturbations this changes. As Δ keeps increasing, the speed of gravity reaches a maximum and then begins to fall back to the c_{em} value. This is slightly noticeable on the blue and yellow curves of the example, where Δ was limited to be less than 1, but it was verified to be the case even for the other curves if larger perturbations were allowed. In conclusion, for high enough momentum or perturbation the difference in propagation speeds between gravity and electromagnetism reduces to 0. The most important differences occur at low q.

The previous results were obtained for a very low hierarchy ($y_- = 2$). As y_- is increased, the shape of the curves in figure 4.3 remains more or less the same except that the interesting features are occurring at lower and lower q, for the same range of Δ, and the differences in speed are decreasing in magnitude. Figures 4.4 and 4.5 show respectively the approximate value of the momentum below which behavior similar to the one shown in figure 4.3 is expected, and the order of magnitude of the maximum relative difference in speeds between gravitons and photons ($\Delta = 0.3$ was kept constant). At $y_- = 2$, the maximum relative differences between gravity and electromagnetism is of order 0.1%, while at $y_- = 10$ this is of order 1×10^{-8}%. Starting near $y_- = 10$ the computation is attaining its practical limit. From an extrapolation based on the fact that the effects decrease exponentially with y_-, it is found that at $y_- \approx 10\pi$, the maximum relative differences between gravity and electromagnetism is of order 1×10^{-27}% and the value of q at which we would begin to see such a small difference is about 1×10^{-13}, in units of k. In this case where the physical brane has positive tension, $k \approx M_{\mathrm{Pl}}$; this means that the interesting momenta are suppressed to near the TeV scale, making them more accessible. The origin of the exponential suppression for the differences of speed is readily understood. Equation (3.57) goes like $\hat{Q}^2 e^{4ky_-}/\hat{r}_0^6$ at large y_-. But $\hat{Q}^2/\hat{r}_0^6$ goes like $e^{-6ky_-}\Delta$. Consequently, $(v_{\mathrm{grav}_0} - c_{\mathrm{em}})$ goes like e^{-2ky_-}, since the perturbation Δ is the quantity that was kept constant while y_- was increased.

In the other case where the physical brane is the negative tension one, the analog of the graph 4.3 is shown in figure 4.6. The numerical results follow the perturbative ones (3.61) very closely. The magnitude of the effect is more important in this case, being of the order of 20% approximatively for $\Delta \approx 0.5$, and this time the speed of gravity is less than that of light. The q-dependence is very weak while increasing Δ has the effect of increasing the difference of speeds. Contrary to the previous case, as higher hierarchies are generated, the magnitude of the effect does not change. This can be seen from equation (3.61) where the dominant contribution goes like $-\hat{Q}^2 e^{6ky_-}/\hat{r}_0^6$, *i.e.* exactly as Δ, which was kept constant. It follows that the difference in speeds also remains constant.

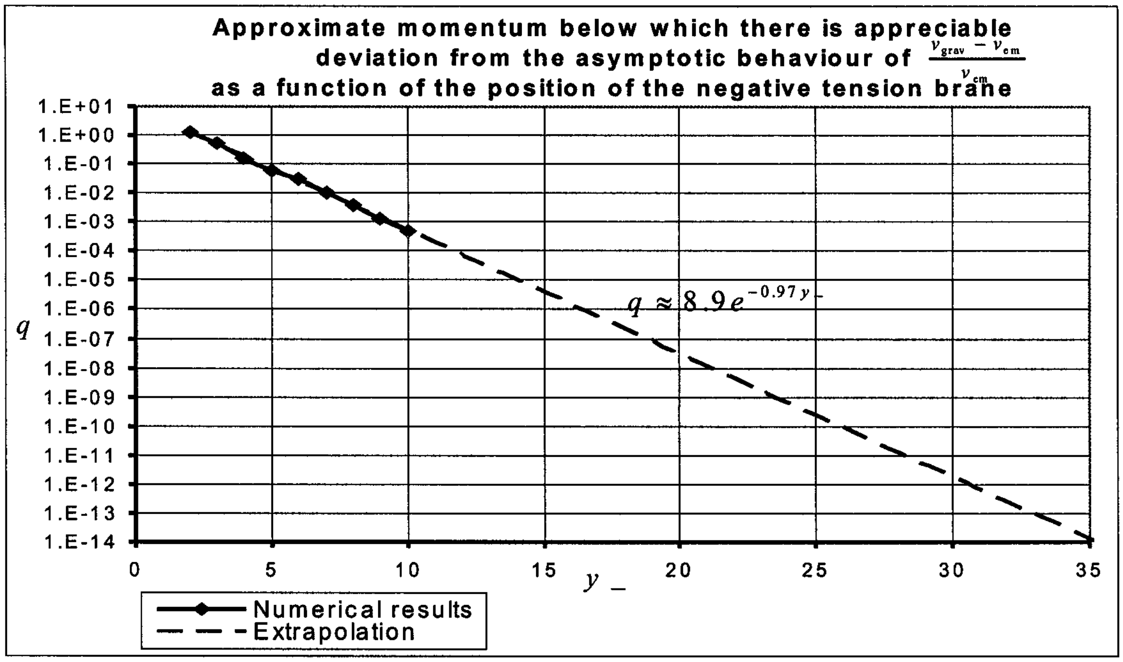

Figure 4.4: Log-plot showing the effect of the hierarchy on the range of interesting momenta when the physical brane has positive tension. $\Delta = 0.3$ was kept constant.

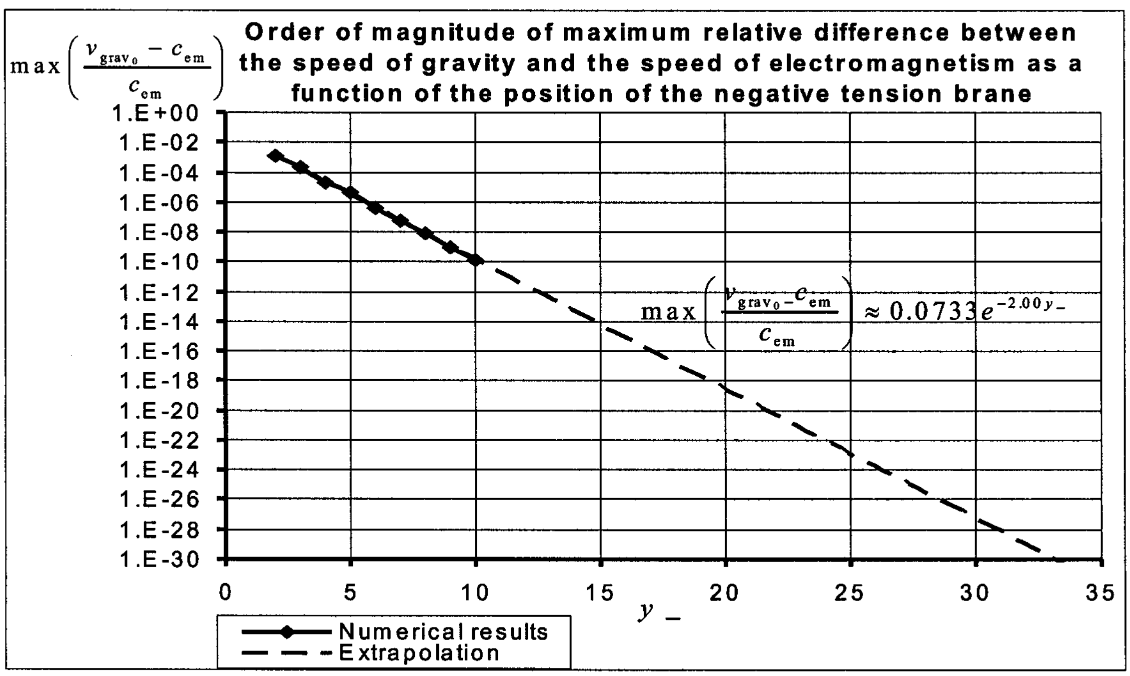

Figure 4.5: Log-plot showing the effect of the hierarchy on the maximum speed difference when the physical brane has positive tension. $\Delta = 0.3$ was kept constant.

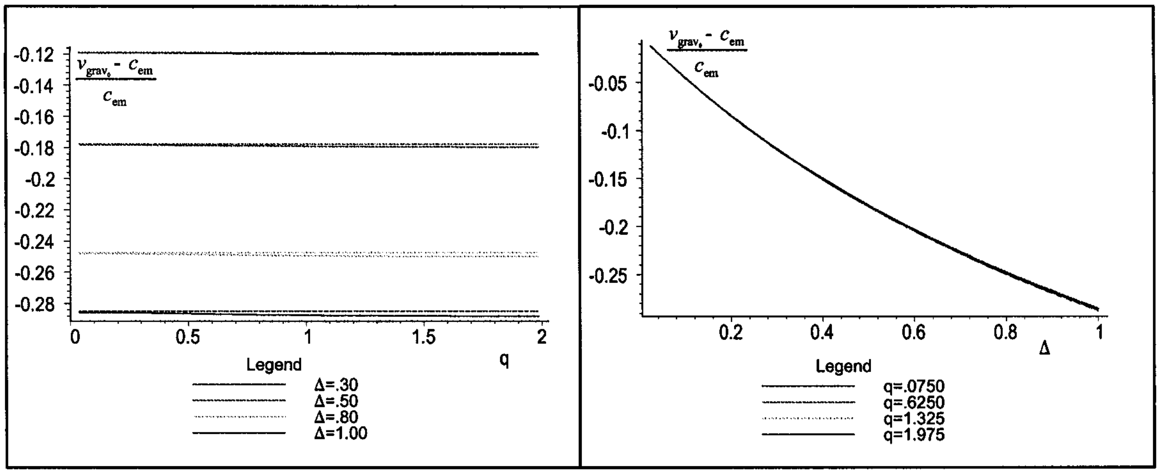

Figure 4.6: Relative speed difference between the gravity zero mode and the photon as a function of q and Δ when the physical brane has negative tension. The dotted lines show the perturbative prediction derived from (3.61), while the solid lines show the numerical result. Each color represents a different perturbation or momentum, and $y_- = 2$.

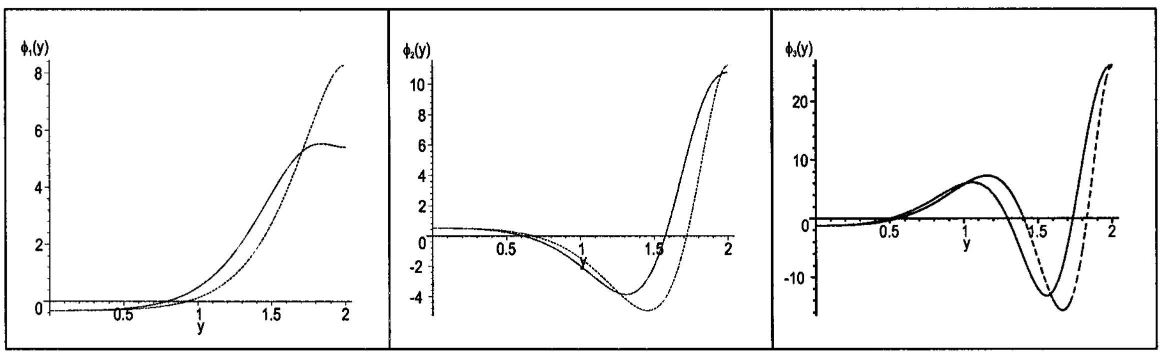

Figure 4.7: Excited states wave functions for the first (left), second (middle) and third modes (right). The blue curves show the unperturbed solutions and the red ones show how the true (numerical) solution behaves as a result of the perturbation. Here $y_- = 2$, $q = 1$ and $\Delta = 1$ for each plot.

4.2.2 *Excited Modes*

Now, passing to the excited modes, we do a similar analysis. Figure 4.7 shows that the wave functions of the first three excited states change less dramatically than for the zero mode, even for a large perturbation. It is interesting to compare with figure 3.2 showing the wave functions of the unperturbed problem at a large hierarchy.

Figure 4.8 shows the correction to the energy eigenvalue. As it should, the perturbative result agrees with the numerical one at low perturbations. The agreement also seems better at low q, but it is a less important effect than for the zero mode case. In particular, the fact that the first order correction to the energy is greater than the true correction for $q = 0$ implies that (3.86) overestimates the mass of the excited modes. At higher momentum, the curvatures of the lines representing the first order result and the numerical one do not even agree, showing the limitation of the perturbative approach. The discrepancies also increase with the number of the mode. The first mode results are fairly concordant under soft perturbations, but for the third mode this is less the case.

As for the speed of the excited modes, figure 4.9 shows, for matter on the positive tension brane, how it compares with that of a similar electromagnetic particle with equal momentum. There is general agreement at low perturbations. As the perturbation is increased, the difference in speeds first rises, but then eventually falls back, contrary to the first order result. Here it is not necessarily true that low momentum gives us better agreement. There seems to be an intermediate range of momentum where the pertubative curves are closer to the numerical ones. As the momentum is increased, the difference between the speeds of the excited states and the electromagnetic particles decreases. Unfortunately, we cannot say what are the asymptotics at large q because it is very difficult to calculate beyond $q = 3$. However, the first mode (blue curves) shows an interesting behavior: at sufficiently high q and large Δ, v_{em} becomes greater than v_{grav}. It would be interesting to know if it is maintained at high q. A similar change of sign in the difference of speeds was found for the second mode for larger momentum and perturbation (not shown). It is probable that this is a general feature for all the excited states.

The difference in speeds was expected to increase with the number of the mode as the scale of the different graphs shows. The numerical results demonstrate, however, that the contrary is happening. The higher the mode, the closer v_{grav} is to v_{em}. For example, concentrating on the blue curves of the graphs that show the dependence on q, the perturbative results suggests that the relative speed difference peaks at about 0.36 for the first mode, at 0.44 for the second, and at 2.00 for the third; the numerical results demonstrate another tendency since the peak values are about 0.22, 0.18 and 0.15, respectively.

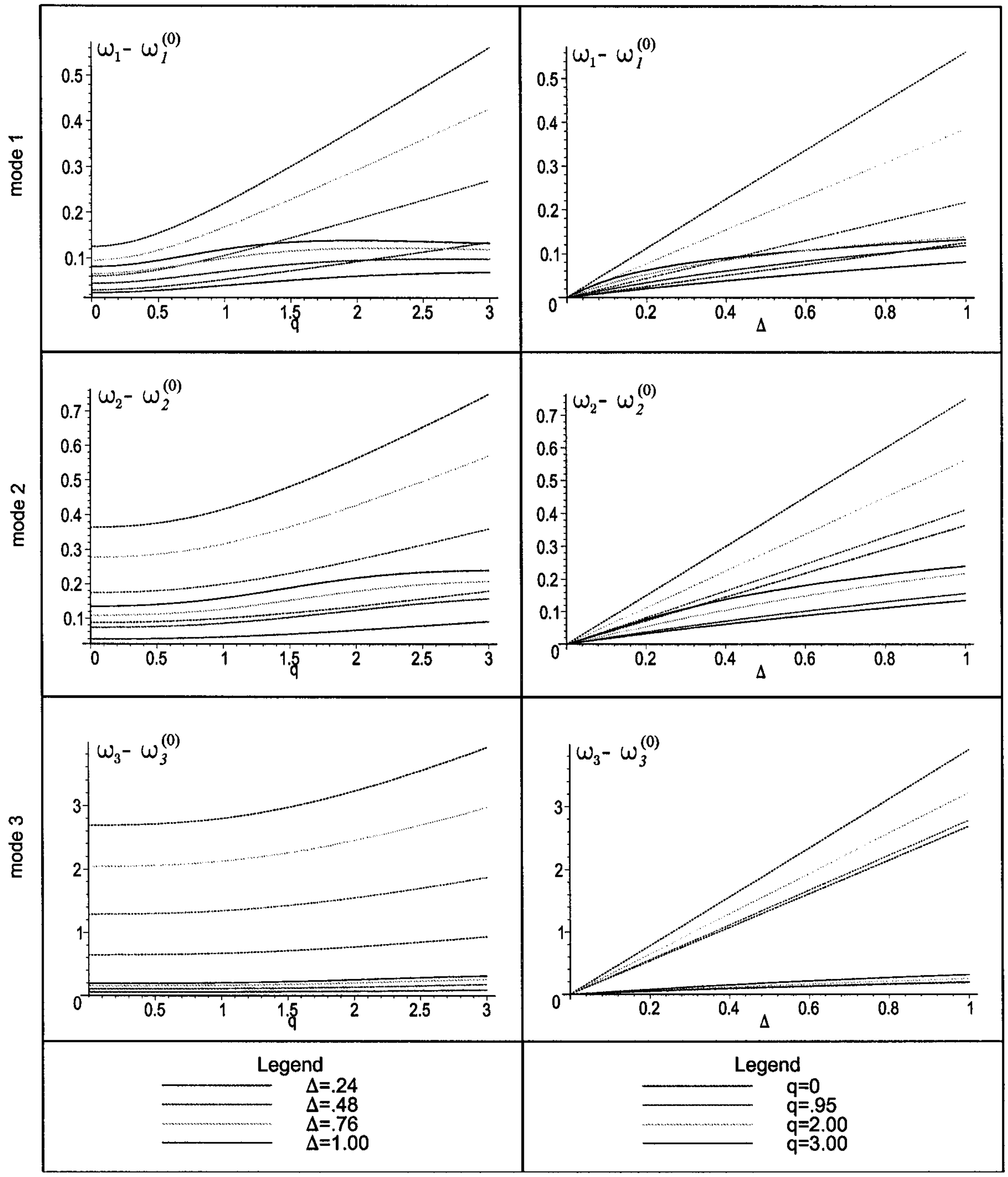

Figure 4.8: Correction to $\omega_n^{(0)}$ as a function of q and Δ. The dotted lines show the perturbative prediction (3.79), while the solid lines show the numerical result. Each color represents a different perturbation or momentum, and $y_- = 2$.

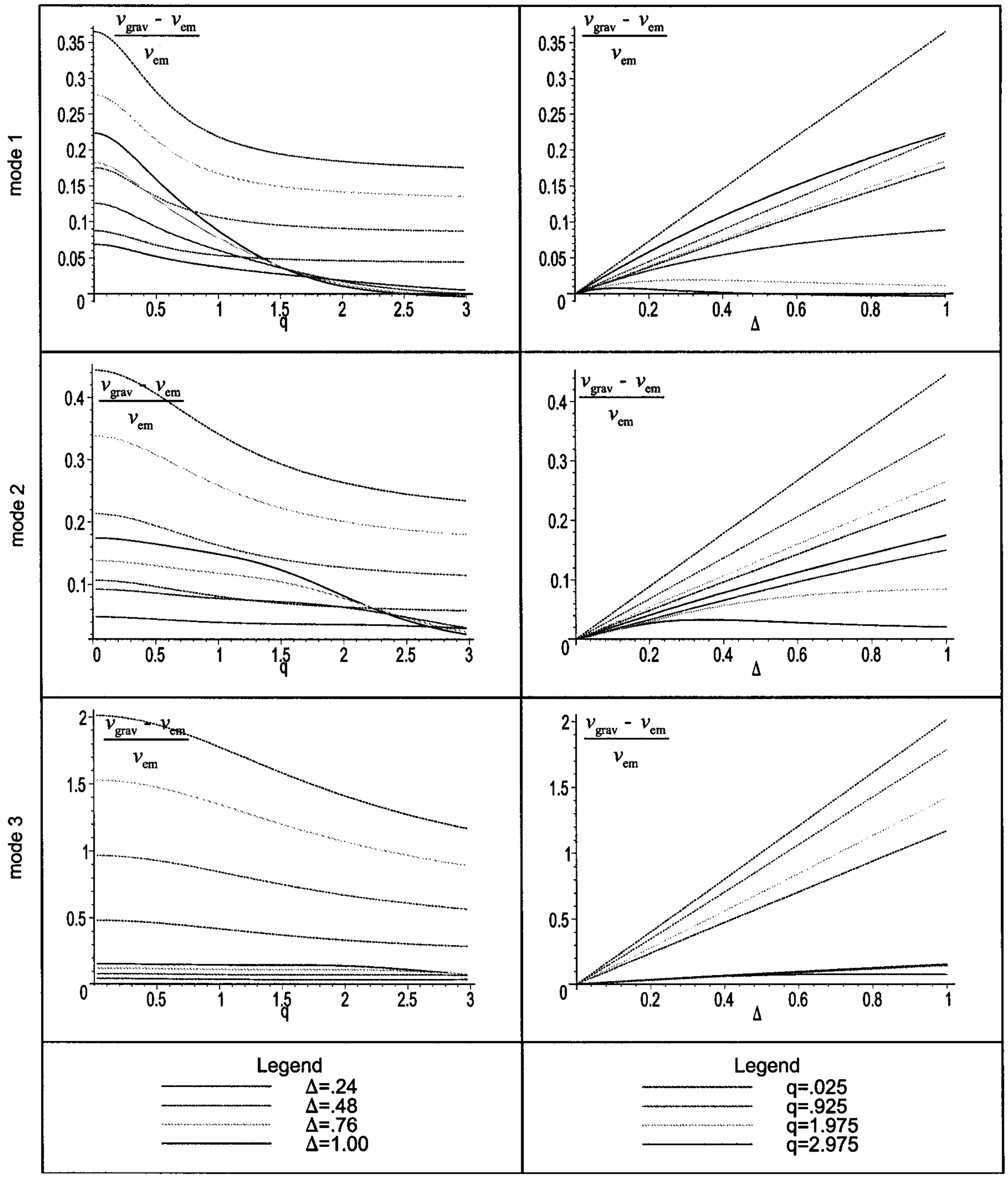

Figure 4.9: Relative speed difference between the gravity excited modes and electromagnetic particles of the same masses as a function of q and Δ. The dotted lines show the perturbative prediction derived from (3.88), while the solid lines show the numerical result. Each color represents a different perturbation or momentum, and $y_{-} = 2$. The physical brane is taken to be the positive tension one.

When the standard model particles are confined to the negative brane, results are quite different. As for the zero mode, the speed of electromagnetism is greater than that of gravity. The magnitude of the effect, though, is comparable with the results obtained on the positve brane. When the momentum is increased, $v_{\text{grav}} - v_{\text{em}}$ reaches a local maximum and then slowly grows to more negative values, which is not shown by the perturbative approach. It also decreases monotonically with Δ. For the third mode, the perturbative result is almost exactly the opposite of the numerical one. This could suggest a sign error in the program, but it is refuted by the good agreements for the first two modes. What happens is that the perturbative curves come from $(v_{\text{grav}})_{\text{perturbative}} - (v_{\text{em}})_{\text{perturbative}}$, where there is an error in each of the two quantities. Although it can be verified that, individually, $(v_{\text{grav}})_{\text{perturbative}}$ is close to $(v_{\text{grav}})_{\text{numeric}}$ and $(v_{\text{em}})_{\text{perturbative}}$ is close to $(v_{\text{em}})_{\text{numeric}}$, the error on each quantity is acting in a different direction; $(v_{\text{grav}})_{\text{perturbative}}$ is overestimated and $(v_{\text{em}})_{\text{perturbative}}$ is underestimated. The errors for this mode are enough to change the sign of the combined quantity $(v_{\text{grav}})_{\text{perturbative}} - (v_{\text{em}})_{\text{perturbative}}$ whereas this does not happen for the previous modes. This shows a limitation of the perturbation method, and it is best then to ignore the third mode results.

For the excited states we did not try to extend the results for greater hierarchies, the computations being too expensive to perform.

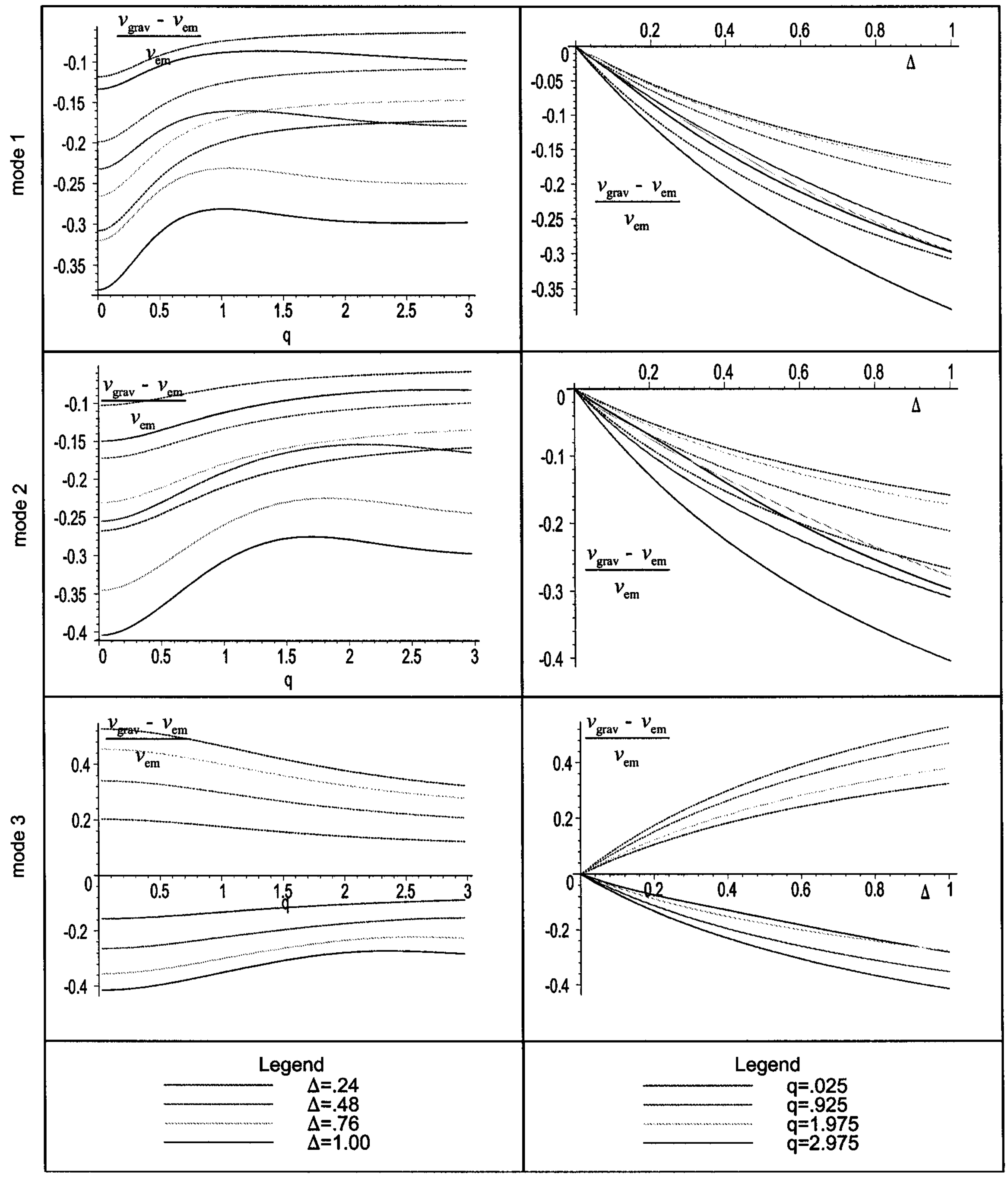

Figure 4.10: Relative speed difference between the gravity excited modes and electromagnetic particles of the same masses as a function of q and Δ. The dotted lines show the perturbative prediction derived from (3.88), while the solid lines show the numerical result. Each color represents a different perturbation or momentum, and $y_- = 2$. The physical brane is taken to be the negative tension one.

5

Physical Bounds on Gravitational Lorentz Violation

Experimentally measuring the speed of gravity is certainly not an easy task. The latest attempt tried to take advantage of the rare Jupiter-QSO encounter that occurred on September 8, 2002 [39]-[41]. However, the result, which was stated as $c_{\text{grav}} = (1.06 \pm 0.21)c_{\text{em}}$, generated controversy among certain members of the scientific community who claimed that the measurement was wrongly interpreted and that it measured nothing more than the speed of light itself (see [42] for example). This, and the examples that follow, show that it requires good precision data and plenty of imagination to obtain some bound for the speed of gravity. In this section, we discuss how the results we found compare with bounds obtained from experiments and from other phenomenological studies, and how they might be applied. We ignore the above result of Kopeikin and Fomalont because of the controversy it faces and because its uncertainty is too high anyway compared with other existing bounds.

There exists an interesting indirect bound from observation of ultra high energy cosmic rays. In the case where gravity propagates slower than light, it is expected that gravi-Čerenkov radiation would dissipate the energy of a cosmic particle traveling faster than the graviton. Hence, observation of high energy cosmic rays coming from astronomical distances implies that such a process is working very inefficiently, from which it is possible to deduce a limit for the speed of gravity. The very stringent bounds obtained in this way in [44] are $(c_{\text{em}} - c_{\text{grav}})/c_{\text{em}} < 2 \times 10^{-15}$ for an observed 3×10^{11} GeV proton of galactic origin and $(c_{\text{em}} - c_{\text{grav}})/c_{\text{em}} < 2 \times 10^{-19}$ if the observed particle was of extra-galactic origin. Since, in the model we investigated with our world on the positive tension brane, we did not find that the speed of gravity could become slower than that of light for the zero mode we conclude that Čerenkov radiation is not possible for this state. Thus we get no interesting constraint in this case. However, it was shown that $v_{\rm grav} < v_{\rm em}$ for large enough q and Δ, at least for the first and second mode, and presumably all excited modes. This permits gravitational Čerenkov radiation into the higher modes if the initial particle is energetic enough to produce massive gravitons that have more momentum than energy. This is probably possible in our model since the massive states have a relatively low TeV splitting and the momentum at which the speed of gravity becomes less than that of light is exponentially suppressed for strong warping, which would correspond to the TeV scale. Unfortunately, radiation of the massive modes was not discussed in detail in [44] so it is difficult to infer a minimum energy for this to happen, but it was mentioned that including them would strengthen the previous bounds by several orders of magnitude. A calculation involving only the excited states would be relevant to our case.

In the other case, where we live on the negative tension brane, the speed of gravity was shown, in our model, to be less than $c_{\rm em}$, even for the zero mode. Thus the bound of [44] can be applied. Even though it is not entirely clear that the perturbative result (3.61) is valid in the momentum range characteristic of the cosmic ray's graviton radiation (because the bound applies to gravitons or KK states with phase velocity $\omega/q < c_{\rm em}$ for $q \sim 10^{11}$ GeV), we still use this approximate result in order to constrain the model; the correct way of constraining the model would require computations impossible to perform. Furthermore, the good agreement between the perturbative result and the numerical one for an observer on the negative tension brane make the use of the perturbative result plausible. Conservatively using the less stringent bound, which is still a far smaller effect than those considered in figure 4.6 and contributes to justifying the use of the perturbative result (3.61), one can deduce that $\Delta < 16 \times 10^{-15}$. Here the Kaluza-Klein gravitons are also slower than their electromagnetic counterpart, even for low momentum, and their spectrum also has a TeV splitting. Thus the excited modes are likely to play a role in the Čerenkov effect. Again, a more detailed calculation is in order for us to deduce constraints on our parameters [1].

For the excited modes, it is unlikely that we would observe any of their Lorentz-violating effects in accelerator experiments if our brane has positive tension. If we can expect the same kind of exponential suppression of the results as for the zero mode for the strongly warped case (which seems quite likely, though we have not proven it), then the effects will not be observable because they will be far too small. On the other hand, the effect might be large enough in the weakly warped case. But in this case the gravitons would have Planck-suppressed couplings and their production cross section will be far too small. If we live on the other brane, the situation becomes more interesting. Now the gravitational resonances are of order of a TeV with TeV-suppressed couplings. It is thus likely that a few low lying modes could be produced at the Large Hadron Collider (LHC). The Lorentz violating effects we found for the zero mode were not suppressed by the effect of warping; if that also applies for the excited states then the effect might be detected in heavy graviton decays. Another possibility where the massive states could be relevant is if they are relics from the big bang. If they are light enough, they could still be around today, but that is probably unlikely. For the rest of the discussion, we will concentrate on the massless state.

For the case where gravi-Čerenkov radiation is not possible ($c_{\rm grav} > c_{\rm em}$), the existing bounds are less stringent. The most direct one comes from the observation that the Sun's spin axis is closely aligned with the solar system's planetary angular-momentum vector and the assumption that this is not coincidental [46]. If there were preferred frame effects, then there would be a torque acting on the Sun that would modify this alignment. Since the measured misalignment is very weak, after the hypothetical torque has been acting during the 5 billion years of the Sun's existence, it is possible to constrain the α_2 parameter of the parametrized post-Newtonian (PPN) formalism that is used to discriminate between the various metric theories of gravity [47]. In turn, this parameter is interpreted as the relative difference in speed

[1]Following the initial submission of this thesis, an investigation of the KK modes in the context presented here was undertaken by James Cline. The results are presented in [45].

between electromagnetic and gravitational waves in the context of Rosen's bimetric theory of gravity. The bound obtained is $|(c_{\text{grav}} - c_{\text{em}})/c_{\text{em}}| \leq 10^{-6}$. Since the experiment constrained the low momentum range and the bound indicates that the speed difference is relatively small, it is then tempting to assume that the small perturbation regime is valid and that the result (3.57) can be used to constrain our parameter. The result is $\Delta \leq \frac{2e^{4ky_-}}{\cosh(2ky_-)-1} \times 10^{-6}$. Both for strong warping and very small warping this gives unacceptably large bounds on Δ that cast serious doubts on the validity of using the perturbative result in this case. Only for a moderate warping might one obtain a respectable bound that would imply $\Delta \ll 1$. For example, with $ky_- = 2$, which is the value used in most of the graphs that were presented, one obtains $\Delta \leq 2 \times 10^{-4}$. It is possible to obtain other bounds, from the numerical results, that do not rely on the perturbative regime and that could also constrain the momentum, but these are complicated to obtain; more computations would be needed. The situation is easier if we live on the negative tension brane. The bound is $\Delta \leq 8 \times 10^{-6}$, valid for any warping except the very low ones, which are not of interest in this model.

Other bounds, more stringent than this solar system test, are obtainable in a somewhat more indirect way. The idea is to study the way in which gravitational Lorentz violations in a brane-world picture influences the dispersion relations of 4D observable particles through graviton loops [48]. The very strong limits on the Lorentz violating effects of ordinary particles [15] then restrict the possibility that the speed of gravity differs from that of light. The authors of [48] obtain various bounds for the different processes under study. The most stringent ones come from atomic spectroscopy constraints and from ordinary Čerenkov radiation from protons in high-energy cosmic rays. Their results are derived for applicability to various scenarios of extra dimensions and depends on M_5, the value of the fundamental scale of the theory. In the 5 dimensional case they are $|(c_{\text{grav}} - c_{\text{em}})/c_{\text{em}}| \leq 3 \times 10^{-15}(M_5/\text{TeV})^3$ and $|(c_{\text{grav}} - c_{\text{em}})/c_{\text{em}}| \leq 1 \times 10^{-17}(M_5/\text{TeV})^{\frac{3}{2}}$, respectively. The first bound is stronger than the solar system one if $M_5 < 700$ TeV, while the second requires $M_5 < 2 \times 10^7$ TeV. For our first case, $M_5 \sim M_{\text{pl}} = 10^{16}$ TeV, so none of these bounds is interesting compared to the previous one. However, for the warped 5D scenario meant to solve the hierarchy problem, $M_5 \sim$ TeV, and these results constitute a marked improvement over the direct bound. The constraints on our model are $\Delta \leq 24 \times 10^{-15}$ and $\Delta \leq 8 \times 10^{-17}$, respectively, again assuming that the perturbative result is applicable (that is disputable, as previously discussed for the Čerenkov bound, since it is again the UV limit of the theory which is relevant here).

Still, the most direct and obvious way to test gravitational Lorentz violation awaits the possibility of performing the experiment. The method consists in comparing the arrival times of a gravitational and an electromagnetic signal coming from the same source [43]. The event could be, for example, a supernova explosion. The gravitational wave would possibly be detected by the recently constructed LIGO detector (Laser Interferometer Gravitational-Wave Observatory). Making some necessary assumption about the relative times of emission of the two signals, the propagation speed of gravity can be deduced. Type II supernovae within a distance of about 20 Mpc, the distance to the Virgo Cluster, are expected to yield a sufficiently strong signal for detection, if the collapse is non-axisymmetrical [49]. For such a distance, and assuming that $\Delta t \leq 5$ yr is the maximal allowable difference of arrival times between the two signals to allow us to identify that they come from the same source, it can be shown that we need at least $|(c_{\rm grav} - c_{\rm em})/c_{\rm em}| \leq 10^{-7}$ for the experiment to yield a believable result. This constraint lessens if the supernova explodes closer to us, but these are much rarer compared to the more distant ones which can occur at a rate of about one per year. A lower limit for this technique also exists. If the difference in times of emission for the electromagnetic and gravitational signals is about one hour, then this leads to an equal uncertainty in the propagation time differences, which represents a $\sim 10^{-11}\%$ lower limit on the above quantity. Given the bounds discussed above, the experiment might not detect anything. In particular, our findings from the extrapolation of the zero mode results (matter on positive tension brane) imply that in the strongly warped case the difference of propagation speeds between light and gravity could be of order $1 \times 10^{-27}\%$ for Δ of order unity, which is well below the above lower limit. Such a tiny effect could never be detected by a gravitational wave observatory. The case where we live on the negative tension brane is therefore more interesting for this experiment because the differences in speed for small enough perturbations are more accessible. In [5] and [10], it is argued that detecting even a tiny difference in speed would severely constrain the parameters $\hat{\mu}$ and $\hat{Q}^2$. Although this is probably the case, the study presented here shows that this is not definitive since the Lorentz violating effect are not strictly monotonic functions of the perturbation (at least for the matter on the positive tension brane case), and there could be dependence on the momentum as well (but very slightly because these experiments concern the infrared limit of q). A tiny difference in speed would therefore constrain only part of the parameter space.

6

Conclusions

The braneworld pictures of the RS type offer various possibilities for solving high energy physics problems. One of the most interesting consequences might be that Lorentz invariance is no longer valid in a higher dimensional context where gravity is allowed to probe the bulk. We studied such a possibility by examining in more detail the work in [5].

Section 2 set the stage for the calculations. We demonstrated that the requirements for having a speed of light that differs along the extra dimension is that the metric be asymmetrical. Such a metric could be obtained if graviton radiation off the brane formed a black hole in the bulk. Assuming that the sources consist of a negative cosmological constant, a scalar field and a $U(1)$ gauge field, the result is an AdS-RN hole which is characterized by its mass and its charge. The embedding of the brane in this spacetime with respect to the $\mathbb{Z}_2$ symmetry and the requirements imposed by the jump equations were then discussed. Applying those to the physical brane, and choosing an ordinary equation of state $\tilde{\omega}_0 = -1$, we found, however, that the black hole singularity is unprotected by a horizon. Therefore, a regulator brane was introduced to cut away the divergences. In particular, it was shown that its position could be chosen in such a way as to solve the hierarchy problem. The equation of motion of a scalar field representing the graviton was written down.

In section 3 attempts were made at solving for the graviton wave function and energy. The unperturbed case was solved exactly in terms of Bessel functions, while the perturbed one had an analytic solution only for the zero mode. Nonetheless, we arrived at an expression for the energy of the excited states, but numerical tools were shown to be needed to compute the final result. Still, we demonstrated how the masses of the unperturbed states are expected to change due to the introduction of the bulk black hole, and how the velocity is expected to change with momentum. Our method is different from that of [5], but we showed that we obtain the same result for the zero mode case.

Not contenting ourselves with the numerical calculation of an approximate result, the full exact computation was performed with a powerful algorithm in section 4. The problem proved difficult to tackle even with the numerical techniques. We obtained partial, but interesting results which are compared with those obtained from the perturbation method. For the case where the physical brane is the positive tension one, the general feature is that the Lorentz violating effects tend to disappear at high momentum and large perturbations. This was not expected from the first order results and suggests that it is probably best to perturb to higher order both in the metric functions and in q to exhibit the two effects to a better approximation. Computations done while increasing the interbrane distance showed that the effect is exponentially suppressed at large separations. In the other case where the hierarchy problem was addressed by having conventional matter on the negative brane, the numerical computations showed better agreement with the perturbative predictions. In this case, the interbrane separation has no effect on the magnitude of Lorentz violations. Whereas gravity was shown to propagate generally faster than electromagnetism for the previous case, the opposite is happening in this scenario. The effects on the massive gravitons were also investigated.

By studying current experimental bounds on the speed of gravity in section 5, we deduced some constraints on the parameters of the model. The more stringent one is $\Delta \leq 8 \times 10^{-17}$ derived from ordinary Čerenkov radiation from protons in high-energy cosmic rays. It applies for the case where we live on the negative brane. The other scenario was not so well constrained. We showed however that speed differences of the order of $1 \times 10^{-27}\%$, far below the current limits, for the strongly warped case were possible. Hopes to see any deviation from exact Lorentz invariance are now mostly founded on the observation of gravitational waves from distant sources. The current bounds suggest that the effect is small enough not to cause an unobservably large difference in arrival times between the optical and the gravitational signal. On the contrary, the experiment might be limited by the uncertainties related to the emission times of the two signals. Very small differences in the speed of light and gravity would then not be measurable.

Not only could the detection of gravitational Lorentz violation be a signature for the existence of extra dimensions, but there are suggestions that such an effect could be used to solve other cosmological problems. In [12, 14], the authors reexamine in this context the issue of the horizon problem, the problem of the uniformity of the cosmic background radiation over causally disconnected regions. The idea is that if gravity can go faster than light, then it can cover larger distances in the same time. Thus regions of the universe that were thought to be causally disjoint may actually have been connected by gravity. A careful study in [9] shows however that the effect is probably too weak to work. Another case of interest with some link to gravitational Lorentz violation is the new flatness problem studied in [11, 10]. The problem is to suppress violations of Lorentz invariance on our brane without compromising the universe evolution to an almost exactly flat one. In [50, 51], the effect is extended to braneworlds of six dimensions. Clearly, the idea that there could be different speeds of propagation for gravity and electromagnetism is an interesting one and it deserves further attention in future works.

A

Alternate choice of parameters

The purpose of this appendix is to describe our first attempt at solving for the position, $\hat{r}_R$, and energy density, $\hat{\rho}_R$, parameters of the regulator brane with specification of $\tilde{\omega}_R$. As will be shown, this is an unfortunate choice because it turns out that not any $\tilde{\omega}_R$ is permissible for a given $\hat{\rho}_0$.

Manipulating equations (2.38-2.39) yields an equation whose roots give us the value for $\frac{\hat{r}_R}{\hat{r}_0} = \frac{\hat{r}_R}{\hat{r}_0}(\hat{\rho}_0, \tilde{\omega}_0, \tilde{\omega}_R)$ and another one whose roots give the value for $\hat{\rho}_R = \hat{\rho}_R(\hat{\rho}_0, \tilde{\omega}_0, \tilde{\omega}_R)$:

$$\left(\frac{\hat{r}_R}{\hat{r}_0}\right)^6 \left(1 - \frac{2\tilde{\omega}_R}{1+3\tilde{\omega}_-}\right) - \left(\frac{\hat{r}_R}{\hat{r}_0}\right)^2 \left(1 + \frac{1}{36}\tilde{\omega}_0\hat{\rho}_0^2\right) + \frac{2\tilde{\omega}_R}{1+3\tilde{\omega}_-}\left(1 + \frac{1}{72}(1+3\tilde{\omega}_0)\hat{\rho}_0^2\right) = 0, \tag{A.1}$$

$$\left(1 + \frac{1}{72}(1+3\tilde{\omega}_-)\hat{\rho}_-^2\right)^2 \left(1 + \frac{1}{36}\tilde{\omega}_0\hat{\rho}_0^2\right)^3 - \left(1 + \frac{1}{72}(1+3\tilde{\omega}_0)\hat{\rho}_0^2\right)^2 \left(1 + \frac{1}{36}\tilde{\omega}_-\hat{\rho}_-^2\right)^3 = 0. \tag{A.2}$$

These look a little bit messy, they are simplified by using explicitly our choice $\tilde{\omega}_0 = -1$ and by defining $x := \left(\frac{\hat{r}_R}{\hat{r}_0}\right)^2$ (this definition is a little different from that in the main body of the text) and $y := \hat{\rho}_R^2$. We get

$$g(x) := x^3 - \frac{b}{(1-a)}x + \frac{ab}{(1-a)} \equiv 0 \tag{A.3}$$

and

$$t(y) := y^3 + \frac{1}{\tilde{\omega}_R^3}\left[\frac{1}{4}(1+3\tilde{\omega}_R)^2\hat{\rho}_0^2 - 9(1+6\tilde{\omega}_R - 3\tilde{\omega}_R^2)\right] y^2 \tag{A.4}$$

$$+\frac{36}{\tilde{\omega}_R^3}\left[(1+3\tilde{\omega}_R)\hat{\rho}_0^2 - 36\right] y + 1296\frac{\hat{\rho}_0^2}{\tilde{\omega}_R^3} \equiv 0, \tag{A.5}$$

where

$$a := \frac{2\tilde{\omega}_R}{1+3\tilde{\omega}_R} \text{ and } b := 1 - \frac{\hat{\rho}_0^2}{36}. \tag{A.6}$$

We again need to find the positive roots of degree 3 polynomials $g(x)$ and $t(y)$. Previous experience in section 2.4 show how to deal with those. Here $g(0) = ab/(1-a)$ and $g'(0) = -b/(1-a)$, and the discriminant of $g(x)$ is proportional to $D1 := -\frac{a^2(1-a)-4b/27}{(1-a)^3}$. But conclusions regarding the number of positive roots are more difficult to draw because the coefficient multiplying x and the constant term in $g(x)$ can be either positive or negative, depending on what value of $\tilde{\omega}_R$ is chosen. In the case of $t(y)$, we have $t(0) = 1296\frac{\hat{\rho}_0^2}{\tilde{\omega}_R^3}$ and $t'(0) = \frac{36}{\tilde{\omega}_R^3}\left[(1+3\tilde{\omega}_R)\hat{\rho}_0^2 - 36\right]$. The discriminant is proportional to $D2 := -27(1-b)\tilde{\omega}_R^6 - 108(1-b)\tilde{\omega}_R^5 + -9(18-19b)\tilde{\omega}_R^4 - 4(27-34b)\tilde{\omega}_R^3 - 3(9-19b)\tilde{\omega}_R^2 + 12b\tilde{\omega}_R + b$. At large $|\tilde{\omega}_R|$, $D2$ will be negative while at small $\tilde{\omega}_R$, the sign will be governed by $12\tilde{\omega}_R + 1$. Again, it is difficult to say right away exactly how many positive roots there are.

At least the discriminant gives the total number of roots for these polynomials. Plotting the regions where $D1$ and $D2$ are positive, it is found that they match exactly, which is reassuring since when there are n solutions for $\hat{r}_R$, then there must be correspondingly n solutions for $\hat{\rho}_R$. For the rest of this section, we shall therefore refer to $D1$ and $D2$ simply as D since they contain the same information. The positive and negative regions of D are shown in terms of $\tilde{\omega}_R$ and $\hat{\rho}_0$ in figure A.1. The figure has been further divided in 7 non overlapping regions, for which we discuss the behavior of $g(x)$ and $t(y)$.

Region R1: $D < 0; \tilde{\omega}_R > 0$, there is only one real root.

$g(0) > 0 \Rightarrow$ it is negative for $g(x)$.

$t(0) > 0 \Rightarrow$ it is negative for $t(y)$.

Region R2: $D > 0; \tilde{\omega}_R > 0$, there are three real roots.

$g(0) > 0$; $g'(0) < 0 \Rightarrow$, two of them are positive for $g(x)$.

$t(0) > 0$; $t'(0) < 0$ if $\hat{\rho}_0^2 < \frac{36}{1+3\tilde{\omega}_R}$; $t''(0) < 0$ if $\hat{\rho}_0^2 < 36\frac{1+6\tilde{\omega}_R-3\tilde{\omega}_R^2}{(1+3\tilde{\omega}_R)^2}$, which can be shown to be true in this small subregion of R2 where $t'(0) > 0$ and thus $t(y)$ is curving down. $\Rightarrow$ there are two positive roots everywhere in R2 for $t(y)$.

Region R3: $D > 0; -1/3 < \tilde{\omega}_R < 0$, there are three real roots.

$g(0) < 0$; $g'(0) < 0 \Rightarrow$ only one of them is positive for $g(x)$.

$t(0) < 0$; $t'(0) > 0$ if $\hat{\rho}_0^2 < \frac{36}{1+3\tilde{\omega}_R}$, which is true in this region since $\hat{\rho}_0^2 < 36$; $t''(0) > 0$ if $\hat{\rho}_0^2 < 36\frac{1+6\tilde{\omega}_R-3\tilde{\omega}_R^2}{(1+3\tilde{\omega}_R)^2}$ which we graphically verified to be the case, so $t(y)$ is curving up at this point. $\Rightarrow$ only one root is positive for $t(y)$.

Region R4: $D < 0; -1/3 < \tilde{\omega}_R < 0$, there is only one real root.

$g(0) < 0 \Rightarrow$ it is positive for $g(x)$.

$t(0) < 0 \Rightarrow$ it is positive for $t(y)$.

Region R5: $D < 0; -1 < \tilde{\omega}_R < -1/3$, there is only one real root.

$g(0) < 0 \Rightarrow$ it is positive for $g(x)$.

$t(0) < 0 \Rightarrow$ it is positive for $t(y)$.

Region R6: $D > 0; \tilde{\omega}_R < -1$, there are three real roots.

$g(0) > 0$; $g'(0) < 0 \Rightarrow$ two of them are positive.

$t(0) < 0$; $t'(0) > 0$ if $\hat{\rho}_0^2 > \frac{36}{1+3\tilde{\omega}_R}$, which is true in this region since $\hat{\rho}_0^2$ is positive and the rhs of the inequality is negative in this region; $t''(0) < 0$ if $\hat{\rho}_0^2 > 36\frac{1+6\tilde{\omega}_R-3\tilde{\omega}_R^2}{(1+3\tilde{\omega}_R)^2}$, which was graphically verified to be the case, so $t(y)$ is curving down at this point. $\Rightarrow$ the three roots are positive for $t(y)$.

Region R7: $D < 0; \tilde{\omega}_R < -1$, there is only one real root.

$g(0) > 0 \Rightarrow$ it is negative for $g(x)$.

$t(0) < 0 \Rightarrow$ it is positive for $t(y)$.

Figure A.2 shows the behavior of $g(x)$ in these different regions. The interesting thing to notice is that if $\tilde{\omega}_R$ and $\hat{\rho}_0$ are chosen so that they are in the region R1 or R7, then it is not possible to place a regulator brane, there is no valid solution to the equations (2.38-2.39). Regions R3, R4 and R5 show that it is possible to place a regulator brane at a determined place in the extra dimension. On the other hand, it may come as a surprise that there seem to be two possible places where to put the regulator brane when $\tilde{\omega}_R$ and $\hat{\rho}_0$ are in regions R2 or R6; the choice seems ambiguous. It remains to check that the corresponding values of $\hat{\rho}_R^2$ that one gets when solving the equations are physical before accepting that there may be two places where the regulator brane can be placed for a given $\tilde{\omega}_R$.

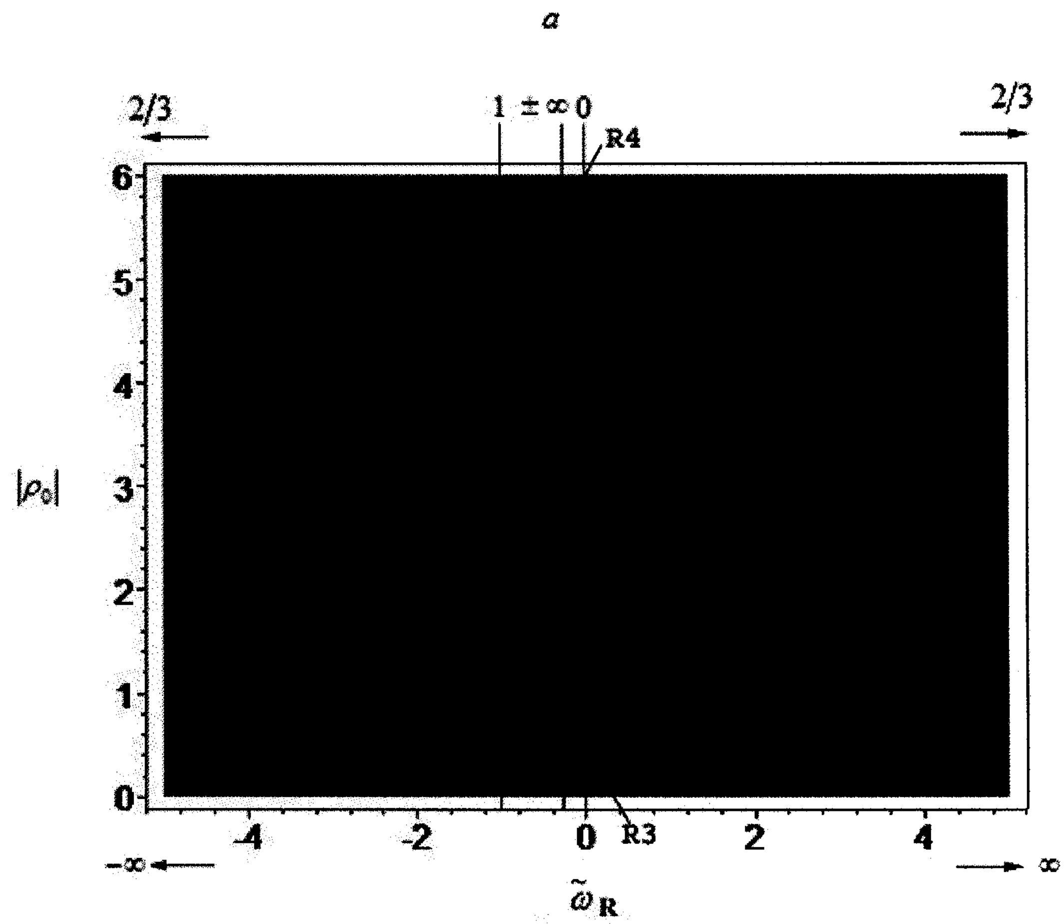

Figure A.1: Regions in red show the place in the $(\tilde{\omega}_R, \hat{\rho}_0)$ space where $D > 0$, regions in blue are $D < 0$.

Figure A.3 shows the behavior of $t(y)$ in the different regions. Again, region R1 has to be rejected for lack of positive roots. This confirms what was found while studying $g(x)$. Here one could think that R7 offers good solutions, but as seen before, it also has to be rejected from the study of $g(x)$. Again, the regions R3, R4 and R5 offer a unique positive solution, which is a good thing because then there is no problem in determining $\hat{\rho}_R^2$. In region R2, there are still two positive roots, which does not invalidate the possibility that there may be two places where to put the regulator brane. Region R6 has three positive roots for $t(y)$ whereas there were only two for $g(x)$. One of these three roots must have no corresponding solution for x and must be rejected. Again, the possibility of having two correct solutions to (2.38-2.39) when $\tilde{\omega}_R$ and $\hat{\rho}_R^2$ are in R6 cannot be invalidated.

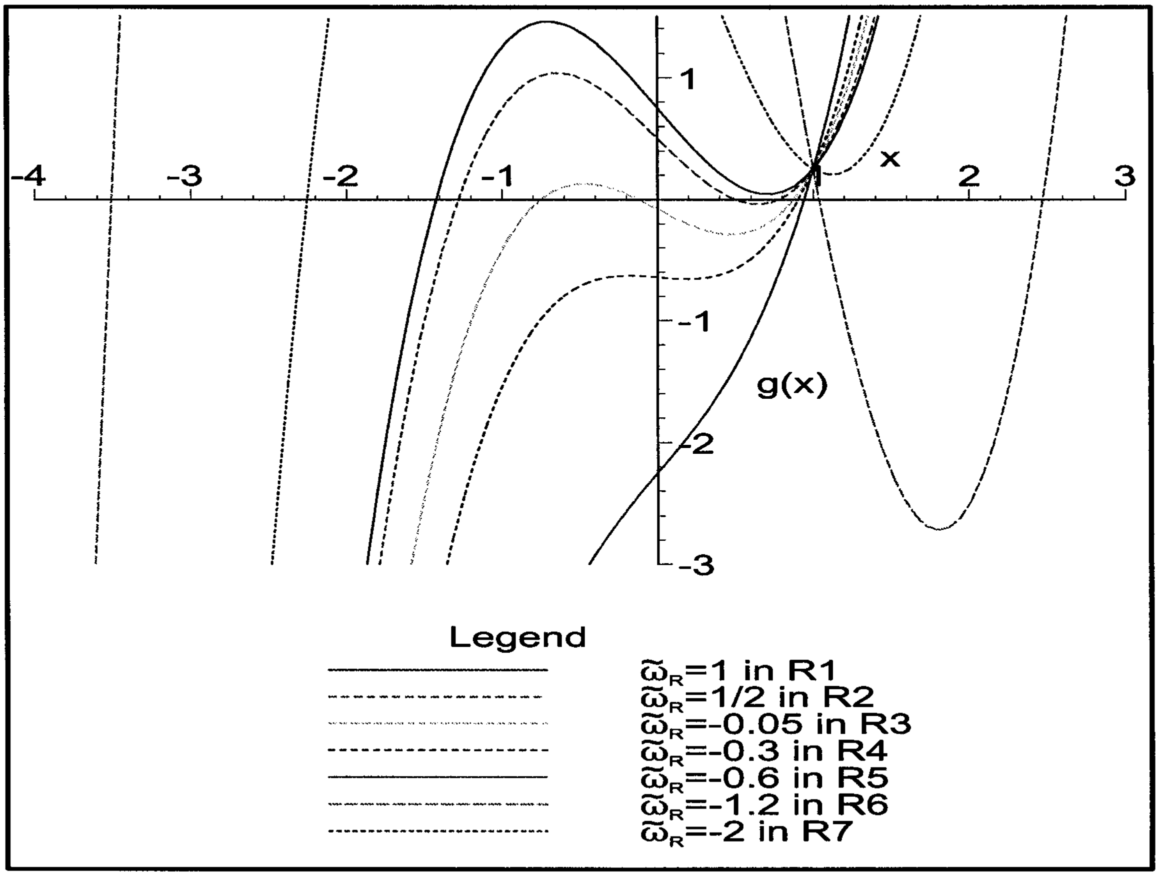

Figure A.2: Behaviour of $g(x)$ for the different regions of figure A.1.

Now that we know what to expect, we can verify that our analysis of $g(x)$ and $t(y)$ was correct and get a better feel for their roots than the one given by figures A.2 and A.3. Plots of the results for $\frac{\hat{r}_R}{\hat{r}_0}$ and $\hat{\rho}_R$ obtained by numerically finding the roots for different values of the parameters $\tilde{\omega}_R$ and $\hat{\rho}_0$ are shown in figures A.4 and A.5 where it is seen that for $\tilde{\omega}_R > -1$, the regulator brane, when it is allowed to exist, will sit between the black hole and the positive brane, and for $\tilde{\omega}_R < -1$, the regulator brane is the outer one. This shows that for $\tilde{\omega}_R > -1$ the energy density of the regulator brane must be negative while for $\tilde{\omega}_R < -1$ it is positive in order to respect the jump conditions discussed before (the outer brane has the positive energy density). The sawtooth pattern on the edges of the graph are numerical artifacts and are smoothed out when a tighter grid is chosen.

The exact predicted behavior is obtained, with the multiple solutions in regions

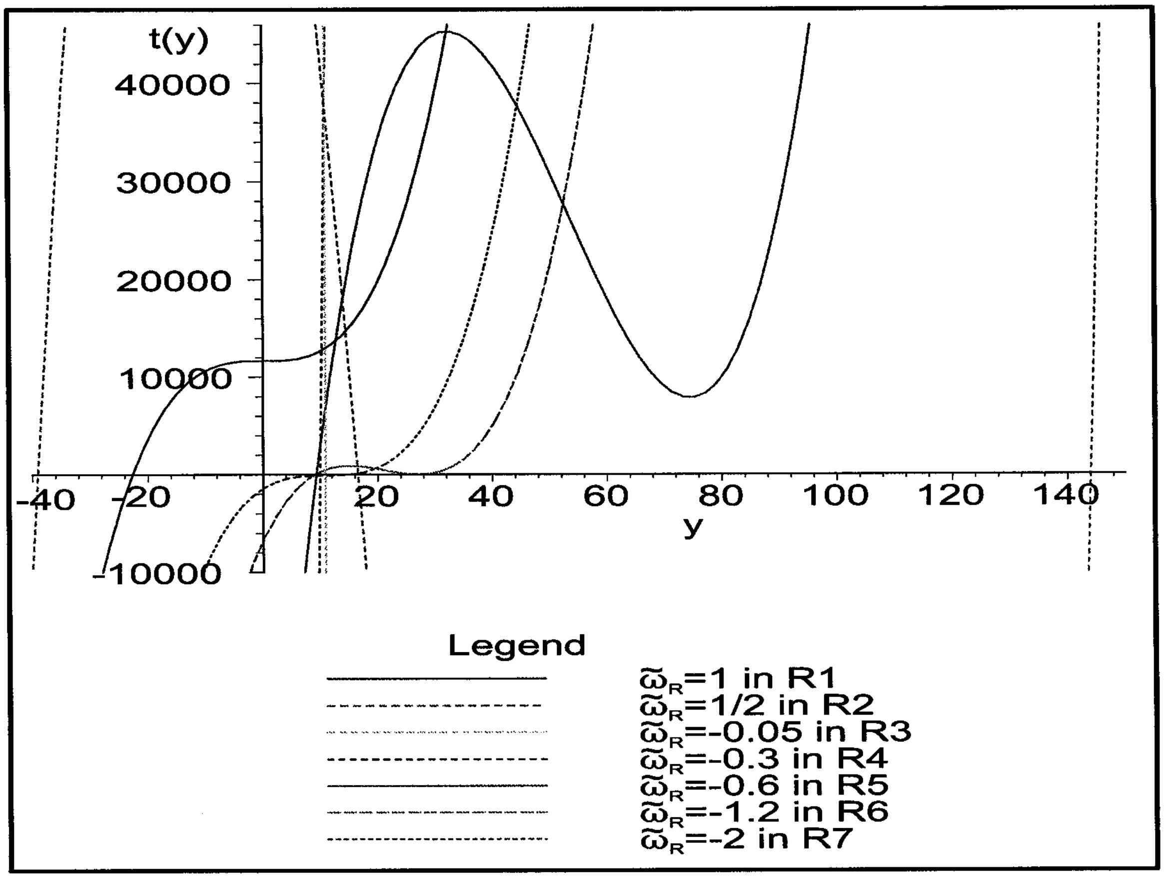

Figure A.3: Behavior of $t(y)$ for the different regions of figure A.1. Note that it has been verified that there are two more negative roots for the curve representing the region R3, as described in the text, but they are too far to the left to be displayed in this graph. The curves for the regions R6 and R7 are also difficult to read with this scale, but zooming in confirms what was said in the text.

R2 and R6. There is, however, a constraint that was not looked at yet, that will eliminate the undesired extra solutions for $t(y)$ in regions R6 and R7, that were discussed previously. Since the equation for the charge of the black hole in terms of the regulator brane parameters is the same as in terms of the physical brane parameters, the same constraint (2.30) applies to $\hat{\rho}_R^2$, *i.e.*

$$\hat{\rho}_R^2 \leq \frac{-72}{1+3\tilde{\omega}_R}, \tag{A.7}$$

when $\tilde{\omega}_R < -1/3$. This constraint is shown in magenta in figure A.5. Any solution above this surface must be rejected. Thus the solution in R7 is eliminated and also the greater solution in R6. The same regions obtained when studying $g(x)$, with the same number of solutions, are recovered. The only thing that remains to do, to verify

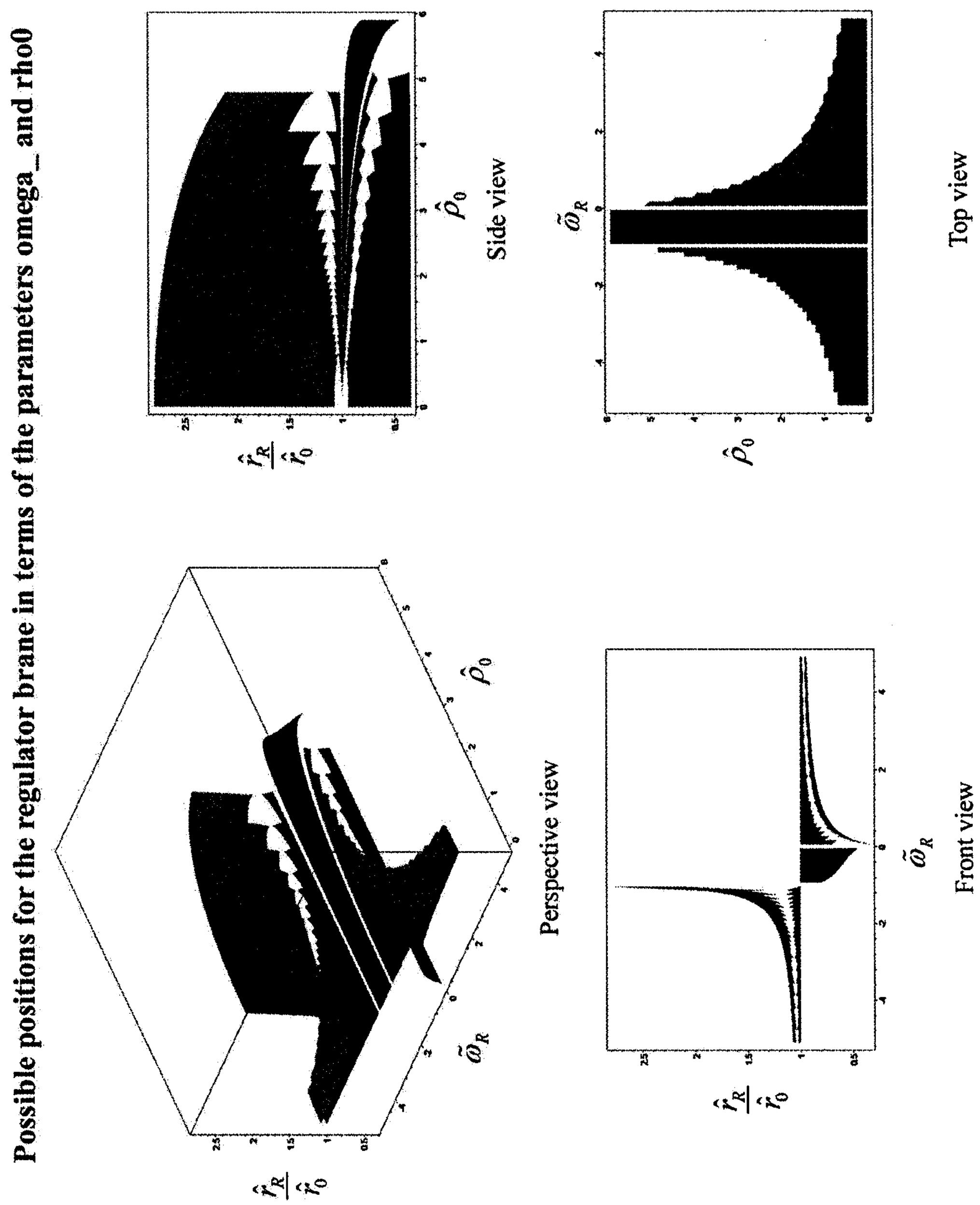

Figure A.4: The possible values of $\frac{\hat{r}_R}{\hat{r}_0}$. When there are two solutions the greater one is shown in green and the lower one in red. When there is a unique solution, it is shown in blue.

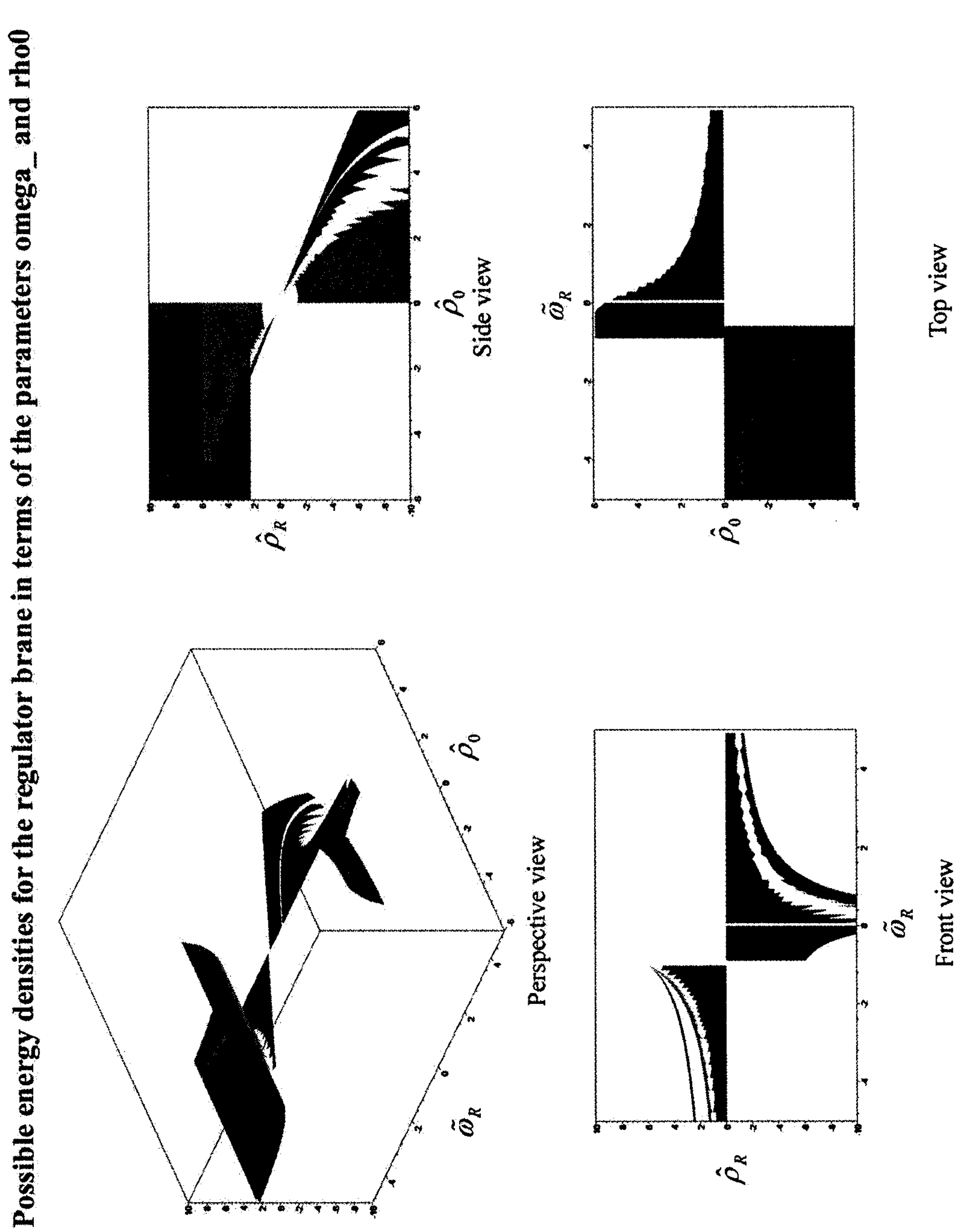

Figure A.5: The possible values of $\hat{\rho}_R$. When there is more than one solution the greater one (in absolute magnitude) is shown in green and the lower one in red. When there is a third solution, the middle one is shown in cyan. When there is a unique solution, it is shown in blue. The magenta surface is $\frac{-72}{1+3\tilde{\omega}_R}$; solutions greater than this have to be rejected because they don't satisfy the positivity of $\hat{Q}^2$. Then there remains no solution in R7 and only two solutions in R6, as it should to be able to simultaneously solve for $\frac{\hat{r}_R}{\hat{r}_0}$ (see previous figure).

that these are correct solutions, is to verify that our solutions can *simultaneously* solve (2.38-2.39). This is not obvious since the equations were decoupled and solved separately, and some solutions were eliminated. It turns out (after verifying with another numerical procedure) that all of the remaining solutions are okay, provided that, in the cases where there is a multiple solution, the lower $\hat{\rho}_R$ solution is taken when the lower $\frac{\hat{r}_R}{\hat{r}_0}$ solution is chosen to form a solving pair, and vice versa.

In summary, $\hat{r}_0$ is arbitrary, $\tilde{\omega}_0 = -1$ is chosen, it was shown that we can choose $0 < \hat{\rho}_0 < 6$ when we choose $\tilde{\omega}_R > -1$ but not in R1, and $-6 < \hat{\rho}_0 < 0$ when we choose $\tilde{\omega}_R < -1$ but not in R7. Then, it is possible to solve for $\frac{\hat{r}_R}{\hat{r}_0}$ and $\hat{\rho}_R$ uniquely when we are in R3, R4 or R5 (blue regions in figures A.4 and A.5). In R2, one can still solve, but there are now two couples of solutions, *i.e.* the green surface in figure A.4 solves simultaneously with the red surface in figure A.5, and vice versa. Similarly in R6, the green surface in figure A.4 solves simultaneously with the cyan surface in figure A.5, and the red surface in figure A.4 solves simultaneously with the red surface in figure A.5.

This way of doing the analysis of the input parameters was a lot harder than what was done in the main part of the text. It can be verified that the conclusions agree. If the 3D graphs of equations (2.42) and (2.41) are plotted, where $\tilde{\omega}_R$ is substituted for x, and rotated in the appropriate way, analogs of figures A.4 and A.5 are recovered. It is unfortunate that taking such a route led to so many difficulties that numerical computations were needed to arrive at our goal, but it nonetheless presented the problem and its solution from another point of view which was valuable because it helped us forge our intuition about the scenario.

BIBLIOGRAPHY

[1] N. Arkani-Hamed, S. Dimopoulos and G. Dvali, *The Hierarchy Problem and New Dimensions at a Millimeter*, Phys. Lett. B429 (1998) 263-272, [hep-ph/9803315 v1].

[2] I. Antoniadis, N. Arkani-Hamed, S. Dimopoulos and G. Dvali, *New Dimensions at a Millimeter to a Fermi and Superstrings at a TeV*, Phys. Lett. B436 (1998) 257-263 [hep-ph/9804398 v1].

[3] L. Randall and R. Sundrum, *A Large Mass Hierarchy from a Small Extra Dimension*, Phys. Rev. Lett. **83**, 3370 (1999), [hep-ph/9905221].

[4] L. Randall and R. Sundrum, *An Alternative to Compactification*, Phys. Rev. Lett. **83**, 4690 (1999), [hep-th/9906064].

[5] C. Csáki, J. Erlich and C. Grojean, *Gravitational Lorentz Violations and Adjustment of the Cosmological Constant in Asymmetrically Warped Spacetimes*, Nucl. Phys. B **604**, 312 (2001), [hep-th/0012143 v2].

[6] C. Csáki, J. Erlich and C. Grojean, *The Cosmological Constant Problem in Brane-Worlds and Gravitational Lorentz Violations*, Gen. Rel. Grav. 33 (2001) 1921-1928, [gr-qc/0105114 v1].

[7] C. Csáki, *Asymmetrically Warped Spacetimes*, [hep-th/0110269 v1].

[8] R. Caldwell, and D. Langlois, *Shortcuts in the fifth dimension*, Phys. Lett. B **511**, 129 (2001), [gr-qc/0103070 v1].

[9] A. - C. Davis, C. Rhodes and I. Vernon, *Branes on the Horizon*, JHEP **0111** 015 (2001), [hep-ph/0107250 v1].

[10] D. J. H. Chung, E. W. Kolb and A. Riotto, *Extra dimensions present a new flatness problem*, Phys. Rev. D65 (2002) 083516, [hep-ph/0008126 v1].

[11] C. Deffayet, G. Dvali, G. Gabadadze and A. Lue, *Braneworld Flattening by a Cosmological Constant*, Phys. Rev. D64 (2001) 104002, [hep-th/0104201 v1].

[12] D. J. H. Chung and K. Freese, *Can Geodesics in Extra Dimensions Solve the Cosmological Horizon Problem?*, Phys. Rev. D62 (2000) 063513, [hep-ph/9910235 v2].

[13] G. Kälbermann and H. Halevi, *Nearness Through an Extra Dimension*, [gr-qc/9810083 v3].

[14] H. Ishihara, *Causality of the brane universe*, Phys. Rev. Lett. 86 (2001) 381-384, [gr-qc/0007070 v2].

[15] S. Coleman and S. L. Glashow, *High-Energy Tests of Lorentz Invariance*, Phys. Rev D **59**, 116008 (1999), [hep-ph/9812418 v3].

[16] F. W. Stecker and S. L. Glashow, *New Tests of Lorentz Invariance Following from Observations of the Highest Energy Cosmic Gamma Rays*, Astropart. Phys. 16 (2001) 97-99, [astro-ph/0102226 v2].

[17] V. A. Rubakov, *Large and infinite extra dimensions: An Introduction*, Phys. Usp. 44 (2001) 871-893; Usp. Fiz. Nauk 171 (2001) 913-938, [hep-ph/0104152 v2].

[18] C. Csáki, J. Erlich, T. J. Hollowood and Y. Shirman, *Universal Aspects of Gravity Localized on Thick Branes*, Nucl. Phys. B581 (2000) 309-338, [hep-th/0001033 v2].

[19] S. Weinberg, *Gravitation and Cosmology: Principles and Applications of the General Theory of Relativity*, John Wiley & Sons, Inc., New York, c1972, pp. 335-338.

[20] P. Bowcock, C. Charmousis and R. Gregory, *General brane cosmologies and their global spacetime structure*, Class. Quant. Grav. **17**, 4745 (2000), [hep-th/0007177 v2].

[21] P. Kraus, *Dynamics of Anti-de Sitter Domain Walls*, JHEP **9912**, 011 (1999), [hep-th/9910149 v2].

[22] S. Forste, Z. Lalak, S. Lavignac and H. P. Nilles, *The Cosmological Constant Problem from a Brane-World Perspective*, JHEP **0009**, 034 (2000), [hep-th/0006139 v2].

[23] C. Barceló, M. Visser, *Living on the edge: cosmology on the boundary of anti-de Sitter space*, Phys. Lett. **B482**, 183 (2000), [hep-th/0004056 v2].

[24] A. Hebecker, J. March-Russell, *Randall-Sundrum II Cosmology, AdS/CFT, and the Bulk Black Hole*, [hep-ph/0103214 v3].

[25] X. Bekaert, N. Boulanger, J. F. Vázquez-Poritz, *Gravitational Lorentz Violations from M-Theory*, [hep-th/0206050 v2].

[26] C. Csáki, *Asymmetrically Warped Spacetimes*, [hep-th/0110269 v1].

[27] J. M. Cline, H. Firouzjahi, *No-Go Theorem for Horizon-Shielded Self-Tuning Singularities*, [hep-th/0107198 v2].

[28] S. M. Carroll, *Lecture Notes on General Relativity, The Schwarzschild Solution and Black Holes*, [http://pancake.uchicago.edu/ carroll/notes/].

[29] P. Hořava and E. Witten, *Heterotic and Type I String Dynamics from Eleven Dimensions*, Nucl. Phys. **460**, 506 (1996), [hep-th/9510209 v2].

[30] P. Hořava and E. Witten, *Eleven-Dimensional Supergravity on a Manifold with Boundary*, Nucl. Phys. **475**, 94 (1996), [hep-th/9603142].

[31] A.-C. Davis, I. Vernon, S. C. Davis and W. B. Perkins, *Brane World Cosmology Without the Z_2 Symmetry*, [hep-ph/0008132 v2].

[32] C. Grojean, *T Self-Dual Transverse Space and Gravity Trapping*, Phys. Lett. **B479**, 273 (2000), [hep-th/0002130 v2].

[33] P. Binétruy, C. Deffayet and D. Langlois, *Non-conventional cosmology from a brane-universe*, Nucl. Phys. **B565**, 269 (2000), [hep-th/9905012].

[34] J. Lykken and L. Randall, *The Shape of Gravity*, [hep-th/9908076 v1].

[35] T. Gherghetta and A. Pomarol, *A Warped Supersymmetric Standard Model*, [hep-ph/0012378 v2].

[36] B. Bajc and G. Gabadadze, *Localization of Matter and Cosmological Constant on a Brane in Anti de Sitter Space*, Phys. Lett. B474 (2000) 282-291, [hep-th/9912232 v2].

[37] W. D. Goldberger and M. B. Wise, *Bulk Fields in the Randall-Sundrum Compactification Scenario*, [hep-ph/9907218 v2].

[38] W. H. Press, S. A. Teukolsky, W. T. Vetterling and B. P. Flannery, *Numerical Recipes in Fortran 77, The Art of Scientific Computing*, Second Edition, Volume 1 of Fortran Numerical Recipes, Cambridge University Press, Cambridge, c1992, pp. 745-774.

[39] E. B. Fomalont and S. M. Kopeikin, *The Measurement of the Light Deflection from Jupiter: Experimental Results*, [astro-ph/0302294 v1].

[40] S. M. Kopeikin, *The Measurement of the Light Deflection from Jupiter: Theoretical Interpretation*, [astro-ph/0302462 v1].

[41] S. M. Kopeikin, *The Post-Newtonian Treatment of the VLBI Experiment on September 8, 2002*, [gr-qc/0212121 v4].

[42] C. M. Will, *Propagation Speed of Gravity and the Relativistic Time Delay*, [astro-ph/0301145 v2].

[43] C. M. Will, *The Confrontation between General Relativity and Experiment*, Living Rev. Rel. **4**, 4 (2001), [gr-qc/0103036 v1].

[44] G. D. Moore and A. E. Nelson, *Lower Bound on the Propagation Speed of Gravity from Gravitational Cherenkov Radiation*, JHEP **0109**, 023 (2001), [hep-ph/0106220].

[45] J. M. Cline, L. Valcárcel, *Asymmetrically warped compactifications and gravitational Lorentz violation*, [hep-ph/0312245 v1].

[46] K. Nordtvedt, *Probing Gravity to the Second Post-Newtonian Order and to One Part in 10^7 Using the Spin Axis of the Sun*, Astrophys. J. **320** (1987) 871.

[47] C. M. Will, *Theory and Experiment in Gravitational Physics*, 2nd edition, Cambridge University Press, c1993, 379 p.

[48] C. P. Burgess, J. M. Cline, E. Filotas, J. Matias and G. D. Moore, *Loop-Generated Bounds on Changes to the Graviton Dispersion Relation*, JHEP **0203**, 043 2002, [hep-ph/0201082 v1].

[49] B. C. Barish, *The Detection of Gravitational Waves with LIGO*, [gr-qc/9905026 v1].

[50] E. Abdalla, A. Casali and B. Cuadros-Melgar, *Shortcuts for Graviton Propagation in a Six Dimensional Brane World Model*, [hep-th/0205203 v1].

[51] E. Abdalla and B. Cuadros-Melgar, *Shortcuts in Domain Walls and the Horizon Problem*, [hep-th/0209101 v2].